IMAGE EVALUATION
TEST TARGET (MT-3)
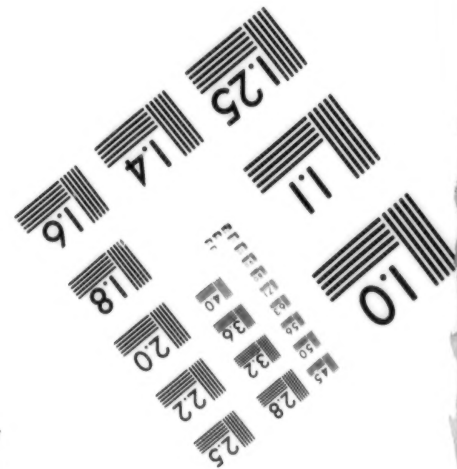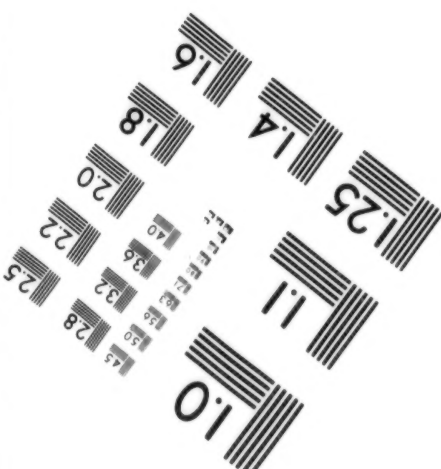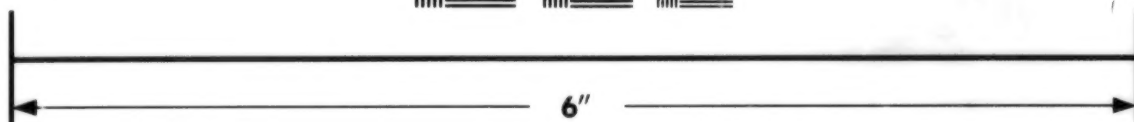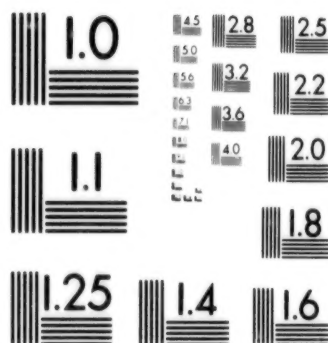
6"
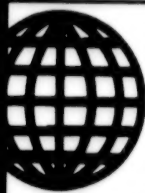
**FOREIGN
BROADCAST
INFORMATION
SERVICE**

JPRS Report

Science & Technology

China

Science & Technology
CHINA

CONTENTS

SCIENCE & TECHNOLOGY POLICY

SCIENTISTS & SCIENTIFIC ORGANIZATIONS

AEROSPACE

ADVANCED MATERIALS

BIOTECHNOLOGY

COMPUTERS

FACTORY AUTOMATION, ROBOTICS

LASERS, SENSORS, OPTICS

MICROELECTRONICS

TELECOMMUNICATIONS R&D

PHYSICS

Report on Third National High-Tech Industries Symposium

Measures for Rectification, Acceleration of Development

90CF0228A Beijing KEJI RIBAO [SCIENCE AND TECHNOLOGY DAILY] in Chinese 18 Dec 89 p 3

[Editor's note by Wu Yunsheng [2976 0061 3932]; article by Deng Shoupeng [6772 1108 7720], analyst, the State Council, Research and Development Center]

[Text] [Editor's note] One of the characteristics of modern-day market competition is that status is acquired through competition and that winning or losing depends on economic strength and scientific and technological ability. In this worldwide competition, both developed nations and developing nations are focusing on advances in high-tech industries in hopes of a better position in tomorrow's world.

China is a developing nation with several decades of experience in high-tech development. A reasonably complete foundation has been formed but large-scale industrialization has not been realized. High-tech has not played a major role in China's development of the national economy and China is still in a weak position in the competition of the world market. Today, the policies of consolidation and reform set by the Party Central Committee and the State Council have placed additional demands on the development of high-tech industries. The current situation is a coexistence of hope and difficulty, and challenge and opportunity. Our ability to create a path for high-tech development that exploits the advantages and suits China's unique situation will have a direct bearing on the realization of China's modernization goal and China's status in the future world. In addition, it also affects the security of the socialist system.

In late November, the Third National Symposium on High-Tech Industrial Development was held in Guiyang under the joint sponsorship of the State Planning Commission, the State Science and Technology Commission, the State Education Commission, the Commission of Science, Technology and Industry for National Defense, and the Chinese Academy of Sciences. The theme of the conference was "bringing the military and civilian sectors together to develop high-tech industries." More than 100 researchers and entrepreneurs from government departments, universities, research institutes, and businesses expressed their opinions. From different perspectives, in-depth discussions were held on the strategy, mode of development, direction, re-structure, and major steps of China's high-tech industry. Printed here are discussions and presentations of some of the representatives at the conference. We hope that more people will pay attention to the development of high-tech industries and contribute ideas for the establishment and development of a high-tech industry unique to China. We shall publish such contributions in the future. [End of editor's note]

—We are facing serious challenges in technology, the economy, education, and organization.

—We must set our strategic target on the general national strength, including economic strength and military strength, and improve economic and social efficiency by combining the military and the civilian sectors.

The pressure of high-tech industrial development experienced by developing nations, including China, is widely known. We are faced with serious challenges in technology, economics, education, and organization. These challenges manifest themselves with the following phenomena. 1) With vast financial and intellectual investments, the developed nations have been able to advance rapidly in the six areas of high-tech—information, new materials, new energy sources, biology, aerospace and marine studies—and have widened the gap between themselves and developing nations. 2) High-tech development in the developed nations has led to the modernization of their whole society and industry, making it very difficult for developing nations to close the gap. 3) Increasing advances in microelectronics, computers, and automation technology have made the traditional industrial and service market rely more on collective know-how and less on labor. The advantages of abundant low-quality labor have eroded. 4) Developed nations have made considerable progress in the manufacture of light, thin, short, and small products; artificial materials; and regenerative energy sources. These developments have greatly decreased their consumption and dependence on natural resources. The situation wherein developing nations have enjoyed the rich natural resources and brisk sales of elementary products has changed. 5) In developed countries education is more popularized and the intellectual and skill levels of the labor force are relatively high; high-tech industry is constantly supplied with qualified workers. In developing countries education is generally backward and the labor force lacks the necessary knowledge and skill; specialist positions in high-tech industry are difficult to fill. 6) In developed countries the severe competition of the market is used in the promotion of high-risk high-tech industries. The fittest survive and the weak are eliminated. In developing countries such a stimulation mechanism has not been formed; high-tech industry lacks vitality and the economic efficiency is low.

The challenge of the six areas above, together with our own economic readjustment, have caused many difficulties for high-tech industry as a whole. Some policy readjustments are needed. For the present time the strategic goal in the development of high technology and industry in China must be in the elevation of the national strength, including economic strength and the military strength. The policy of combining the military and civilian sectors should be adopted to improve the economic and social efficiency of the entire industry. High-tech industries are strongly international; we must make use of foreign capital, technology and talent and develop cooperation in different areas.

The following issues should be considered at this time. 1) During the period of consolidation and reorganization, we should seize the opportunity of industrial-structure readjustment to push high-tech into traditional industries and change the high-tech composition of the major enterprises in traditional industry. 2) Using the available resources, we should combine the three major efforts (the S&T key plan, the "863" plan and the "Torch Plan") into one unified national high-tech industrial development plan. 3) We should promote organizational reform in production. First, select and support a few high-tech enterprise groups from the defense industry system to compete in the international market. Developmental institutions in the Chinese Academy of Sciences and in universities may take their research results that they cannot commercialize themselves and turn them into equivalent stock by participation in joint-venture high-tech product development with foreign capitalists. 4) We should participate in the horizontal distribution of effort of international high-tech industries, and develop OEM type of activity (commissioned production or brand production). Through these activities, the idle labor force in China can be used in creating foreign exchange for the country.

Orientation Toward Service to National Economy

90CF0228B Beijing KEJI RIBAO [SCIENCE AND TECHNOLOGY DAILY] in Chinese 18 Dec 89 p 3

[Article by Gan Shijun [3972 1597 0193], standing deputy director, State Science and Technology Commission, Research Center]

[Text]—High-tech industries should grow out of base industries and join in with national industries in the main economic arena.

—Concentrate resources to form a high-tech industry group and establish an effective international avenue in management and consolidation.

—Promote "Torch Plan" projects and create an environment for innovation in high-tech industries.

High-tech industry is an economic concept characterized by high risk, high growth, concentrated capital, concentrated intelligence, and a fast pace. The primary goal of high-tech is to improve the economic competitiveness of the country.

In improving China's high-tech industry, there are two areas that I consider to be important. One is that high-tech goes with higher management, that is, doing business according to the characteristics of high-tech and the laws of economics. The other is combining high-tech with the real economic situation in China. I also think that we should not view high-tech as music that only appeals to the highbrows. In today's world, high-tech is already a common economic phenomenon and an effective avenue for developing nations to achieve economic prosperity. "The Four Small Dragons" have followed this route, and now Thailand and Malaysia are moving fast on this track.

How are we to combine the development of high-tech industry with China's economic development? There are at least three considerations. First, let high-tech enter the main arena of the national economy, that is, build high-tech on the main thrust of the national economy. High-tech should particularly serve the development of China's basic industries. High-tech should not only reform traditional industries, but should diffuse into traditional industries and create a new generation of basic industries. In this sense, our most urgent need now is not to make large-scale high-tech plans; instead, it is to fold high-tech into the existing economic planning system (not just the science and technology planning system). The state should take action so that high-tech may enter China's industrial structure directly or indirectly.

Second, high-tech industries should form groups and follow an international approach. China is a large and poor country and cannot possibly have a large amount of capital for high-tech development. This is not conducive to the requirement of concentrated capital in high-tech development, but we are totally capable of focusing the national resources to form a few high-tech groups with international competitiveness. Compared to advanced nations, China holds certain advantages in high-tech research, manpower, and equipment. We also have a vast reserve of research results with commercial value, but we have not worked on our competitiveness. I feel that our main problem is the lack of internationalization in our high-tech industries. Without sufficient movement, we cannot import more technology. At the present time we are falling behind mostly in high-tech management, finance, business activity, intermediate connections and management personnel. These shortcomings have severely impeded the development of high technology. A vitally important long-term issue today is how to build up a healthy and effective international channel.

Third, we must create a favorable environment for the development of high-tech industries; we must seek opportunities to develop the vast research results in the various departments into a major business. The state can do a lot in supporting such developmental efforts. The "Torch Plan" is an important event; and it should be more than just a project, it should be first and foremost an innovation plan. Innovation is the driving force behind high-tech. In socialism the state supports the creation of a favorable environment for innovation. The "Torch Plan" is such an effort. While funding projects, it also provides support for new-technology development zones, incubators, and information guidance. The plan also explores avenues to facilitate financial, tax and legal services, and technology transfer, product commercialization, and promotional areas. People may not realize its value now, but before long the "Torch Plan" will play an important role in China's long-term economic development and the industrialization of high technology.

Relations Between Industry, Academia

*90CF0228C Beijing KEJI RIBAO [SCIENCE AND
TECHNOLOGY DAILY] in Chinese 18 Dec 89 p 3*

[Article by Zhang Bihui [1728 4310 2547], associate
professor of the Central China Science and Engineering
University]

[Text]—High-tech industry is the result produced by
combining the intelligence of the universities and
research institutes and the financial resources of
industry. On the international scene, some combinations
have succeeded and others have not. The key is to find
the interface for industrialization.

In terms of the course of development, high-tech enter-
prises are the results of combining the intelligence of the
universities and research institutes and the financial
power of the industrial sector. This is why some new
high-tech development zones in the world are near
universities. Experience has also shown that the success
of high-tech companies and enterprises often is not
based on the proximity to market, an abundance of raw
materials, or a labor force with special skills; instead, it
depends on the acquisition of research results at an early
date. The combination of universities and industries
promotes the development of high-tech enterprises and
economic progress, and helps technology transfer and
product commercialization.

The development of high-tech enterprises and the
economy in China relies mainly on the growth of science
and technology. The necessity and importance are
unquestionable; the question now is how to industrialize
high-tech and how to find the interface for industrializa-
tion. In the cooperation of universities and industry,
some projects have worked very well but there are also
cases where the two sides have blamed and criticized each
other. The universities blamed the industry for not
spending enough money on research and development
and the research results did not receive the proper atten-
tion. The industry blames the universities for results
which lack adaptability and which cannot be used right
away. It is true that our production force is still not fully
developed, the management system has not been com-
pletely worked out, and the ability of industry to absorb
advances in science and technology is relatively weak.
The lack of motivation and pressure to absorb advances
in science and technology has caused a multitude of
problems in technology transfer. But on the other hand,
the universities should not stay in a passive position. Not
every university can develop high-tech industries around
its campus. Oxford University and Cambridge Univer-
sity, both famous universities with 1,000 years of history,
have fared very differently in the wave of high tech-
nology. Around Oxford there is no activity and one
cannot find a piece of land to build a science park; as a
result, it has suffered economic difficulty and lost some of
its people. Cambridge, on the other hand, is surrounded
by hundreds of companies and enterprises and has cre-
ated the famous "Cambridge phenomenon" in economic

development. Both Cambridge University in England
and Stanford University in the United States have pro-
moted the development of high technology; they have
done so with their unique intellectual foundation and
economic and cultural environment. First, they found an
interface for developing industrial cooperation. They
regarded maintaining cooperation between universities
and industries as a traditional duty of the university and
an avenue to elevate academic standards. Next, an eco-
nomic environment attractive to entrepreneurs should be
created. In this regard Western countries made their
effort mostly in providing favorable policies for venture
capital. Finally, there should be a cultural environment,
particularly a creative spirit and an ability to endure risk.
In China, the few universities regarded as more successful
in technological development are also the ones more
successful in the areas just described.

The connection between university and industry has had
a long history. In the development of high-tech, the two
parties should be complementary. Universities should
have the intention to commercialize their research
results and industry should pay attention to the aca-
demic goals of the university and make good use of the
resources of the university. Both sides should take an
active role and work together to join up at the interface.
Only then can we develop our economy based on science
and technology advances and growth.

Concentration on Unified Leadership

*90CF0228D Beijing KEJI RIBAO [SCIENCE AND
TECHNOLOGY DAILY] in Chinese 18 Dec 89 p 3*

[Article by Wang Luye [3769 6424 8763], assistant
researcher, Office of Administrative Research, Commis-
sion of Science, Technology and Industry for National
Defense]

[Text]—Concentrate necessary money and manpower,
create a local development environment to make break-
throughs with a limited number of targets.

—Concentrate unified leadership for an economy dif-
ferent from the singular planned economy of the past.
The central function of the economy is to improve the
operation of the government and to strengthen mac-
roscopic control and service.

In the transition from the simple planned economy to
planned commodity economy and before the market
system is perfected, the purpose of concentrating unified
leadership is mainly to supplement the inadequacies of
the market system. High-tech industry may be divided
into four levels. First, high-tech industry based on the
major sciences; second, high-tech industry characterized
by economies of scale; third, high-tech industry oriented
toward defense; and fourth, high-tech industry based on
market forces. For the first three levels, the unified
leadership of the state should consist of formulating
policies, breaking down barriers between departments,
and optimizing the integration of production means. By
doing so, the limited monetary and manpower resources

will be used at the right places and breakthroughs on the local and professional level can be achieved at an earlier date. For the fourth level, the unified leadership of the state should consist of formulating sound policies and regulations, creating an environment for fair competition and providing services. For the management of the fourth level, China does not have very much experience, especially the management of almost 10,000 small and medium-sized high-tech companies that emerged during reform. In this area we need to learn from the more successful Americans and Japanese. Through formulating correct policies and regulations, we need to create a healthy, fair and creative environment for competition so that industries can move toward the international market and become an important part of China's high-tech economy.

It should be pointed out that concentrated, unified leadership is totally different from the simple planned economy of the past. In today's situation, its central role is to improve the function of the government and macroscopic control. For high-tech industries, we should on the one hand formulate development policies and regulations and on the other hand change direct interference to macroscopic control and service in order to supplement the inadequacies of the present market system. In formulating high-tech development policies, we must follow the following principles. First, correctly handle the relationship between equilibrium and development. Second, improve the efficiency of the market mechanism. Third, make a transition toward the macroscopic level. Fourth, adopt different development policies for high-tech industries at different levels. Macroscopic control also exhibits itself as services; internally it shows up as information guidance, policy guidance, and capital construction, and externally it shows up as services in politics, foreign policy and even in the military. The service function of government resides in concentrated unified leadership. Our government officials must change their thinking and concepts about the long-held planned economy model and change the ideas that have resulted from thousands of years of history.

Shift of National Defense S&T to Civilian Sectors

90CF0228E Beijing KEJI RIBAO [SCIENCE AND TECHNOLOGY DAILY] in Chinese 18 Dec 89 p 3

[Article by Li Yinqi [2621 5593 3217], senior engineer, Shanxi S&T Information Institute]

[Text]—Shift defense S&T to civilian sectors so that it may become a reliable force in China's national and regional high-tech reform and economic development.

To properly shift national-defense S&T to the civilian sectors, we must seriously address the following five combinations:

First, the shift should be combined with the use of military technological power to develop and build up China's high-tech industry. Defense S&T can help high-tech industry with strategic guidance, technical support

(manpower and equipment), product restructure, shift of enterprise category, production and technological management, and information services. Aerospace, nuclear technology, microelectronics and computers, new materials, and bioengineering belong to both defense S&T and high-tech industry. Military resources should be used in the development of outgoing high-tech products (including military products) in order to accelerate the growth of China's high-tech industry.

Second, the shift should be combined with using military technological power to develop major national technological facilities. Examples are multi-purpose satellites, serialization of launch vehicles and entering the international aerospace market; development of nuclear power and isotope technology; development of aircraft for domestic flights; integration of optical, mechanical and electrical technology and its application in traditional fields; providing traditional industries with a new generation of equipment; and bioengineering research in agriculture and medicine.

Third, the shift should be combined with using military technological power to complete major national or industry-wide technological reforms. The goals should be high efficiency, precision, long-life, and automation. Technical reforms should be conducted in the casting and forging, die-making, automotive, energy, chemical and instrumentation industries.

Fourth, the shift should be combined with using military technological power to develop the economy of industrial zones and cities. In Tianjin, Ningbo and Shenzhen, the development of local economy was linked to defense research institutes and institutes of higher learning through a number of channels. By doing so, local economic development has found reliable technical support and backup.

Finally, the shift should be combined with using military technological power to import, digest and absorb advanced technology. In recent years China has imported 231 production lines for large-scale integrated circuits [LSI], computers and color television sets, but only 13 of them are economically viable and can compete in the domestic and international markets. Many efforts to import and absorb advanced equipment and to manufacture such equipment in China have fallen behind. Because of problems in the management system and the high costs of processing, many sets of imported equipment are not sufficiently used and scattered and, as a result, the environment for improving processing capability has not been formed. The cooperation between the defense industry and the civilian sector should be based on proximity and mutual willingness. They should work together to digest and absorb imported technology, to innovate, and to blaze the trail for China's manufacturing industry.

Establishment of Strong Intermediary Organization

90CF0228F Beijing KEJI RIBAO [SCIENCE AND TECHNOLOGY DAILY] in Chinese 18 Dec 89 p 3

[Article by Ye Xilin [0673 6932 2651], researcher of the Economic Management Institute, Ministry of Aeronautics and Astronautics Industry]

[Text]—Military and civilian cooperation is a formidable task and must not be taken lightly.

—Military industrial enterprises should find an equilibrium between the market and technology, and not compete with the civilian sector.

Today, military-civilian cooperation is moving from the most beginning stage to a more advanced new level. The new level should be characterized by exploiting the achievements of military technology over the last 40 years and serving the national economic development.

The two main issues in military-civilian cooperation are: First, modify military products for civilian use. Examples include aircraft for aviation and space, artificial earth satellites and their power devices, guidance systems, electrical instruments, communications components and parts such as valves and switches, and other accessories. Second, transfer military technologies to civilian use. This includes automatic control technology for aviation and space, remote-sensing and telemetry techniques, jet-propulsion technology, low-temperature methods, hydraulic technology, high-pressure-vessel welding technology and new materials.

Because the military industry was closed to the outside for a long time in the past and practiced a highly planned economic system, the military and the civilian industries did not understand each other and the military was not familiar with the market and sales. Therefore, a strong intermediary organization should be established between the departments and the enterprises. The organization should consist of a group of experts familiar with both military and civilian products and specialized in both production and marketing. The main mission of the intermediate organization is to conduct market surveys and forecasts, to communicate between the enterprises and the market, to promote military products for civilian use, and to develop a product market driven by both military technology and user needs.

To this end, we need to establish the following strategy. First, military-civilian cooperation is a complex task that involves many aspects. The space technology of the Soviet Union is very advanced, but its technology transfer to the civilian sector has produced very little. The United States is very experienced with military-civilian cooperation; their technology transfer in the Apollo Moon-Shot Project to the civilian sector involved a large group of experts and several years. Therefore, we should realize the difficulty and complexity of the task and must not take it lightly. Second, in the development of civilian products by the military

industry, the effort should be guided by both the market and technology in order to achieve a dynamic balance between them. One should not consider only the market and ignore the advantages of military technology, nor should one engage in low-tech repetition with the civilian industry. For example, many military industries in recent years blindly jumped into producing refrigerators and color television sets. The military industry should make use of existing technological advantages to develop high-quality, low-cost, technology-intensive new products that can be developed with a short lead time and compete in the domestic and international markets.

Orientation Toward Transforming Traditional Economy

90CF0228G Beijing KEJI RIBAO [SCIENCE AND TECHNOLOGY DAILY] in Chinese 18 Dec 89 p 3

[Article by Gu Shulin [7357 3219 2651], associate researcher of Policy and Management Institute, the Chinese Academy of Sciences]

[Text]—The goal of China's high-tech development should be using high-tech to change China's traditional energy-wasteful, low-efficiency industry and making high-tech an important means and driving force to overcome China's economic difficulties. This is the only choice for developing countries to achieve economic success.

There are a number of problems in China's high-tech development, from the understanding to the practice. One distinct problem is that the development of high-tech and the development of traditional industry are still separate. Looking back on progress in the last few years, the first item that should be brought to the forefront is that the goal of China's high-tech development must be clearly defined. This goal should be using high-tech to change China's energy-wasteful, inefficient traditional industry, and making high-tech an important means and driving force to overcome the difficulties in China's economic development, and to establish a sound relationship between high-tech development and actual economic activity. Such a strategy is a comprehensive strategy combining high-tech and economic development. Basically, this is the only choice for developing nations to develop their economy by the end of the 20th century, when the world will have entered a high-tech age.

To implement this strategy, attention should be given to a series of fundamental high-tech fields that can be interfaced with traditional industry. The criteria for selecting these strategically significant high technologies are: 1) the technology is widely coupled to traditional industry, 2) it can be accepted by current and near-future economic endeavors, 3) it can help solve some of the difficulties in China's economy. This is a series of fundamental technological reforms aimed at improving China's economic structure, efficiency, and adaptability. Examples are industry automatic control and numerically controlled machine-tool technology; electric-power and electronic technologies; high-level technologies for manufacturing; enzyme and

fermentation engineering; genetic engineering; biotechnology with short-term to mid-term applications to agriculture, pharmaceuticals, foodstuffs, and light industry; water-treatment technology that can help China's shortage in water resources; computer-management systems that can improve macroscopic control and management at various levels; and satellite computer education systems that can improve the means for education. Basic high technologies should be given high priority in order to form a sound, in-depth research and development ability and an ability to provide software and hardware in the reform of China's traditional economic structure.

In order to implement such a strategy, new demands will be placed on the central government, local government, departments, major enterprises, and research organizations. The planning of intermediate projects should be done on the basis of lower projects so that an overall high-tech development may emerge and complement the economic development.

To implement such a strategy requires advanced and sophisticated inter-system coordination. In China the high-tech R&D departments and economic departments, including high-tech industrial departments, have all gone through some maturation and became fairly independent "departments." Lack of communication between the departments has been the biggest problem that we have encountered. Every department is trying to develop the entire process of R&D to production. This is not only detrimental to the effective utilization of resources, but also perpetuates the separation between high-tech and traditional industry. High-level comprehensive cooperation between the Chinese Academy of Sciences and the oil and gas industry has been going on for 7 years and has resulted in many achievements satisfactory to both sides. A sensible rights and responsibility relationship is basic to the success of cooperations. Socialistic cooperation with scientific management may be an important organizational avenue for bringing together R&D and production.

Nuclear Industries' 2nd Research Institute Highlighted

90FE0018A Beijing BEIJING KEJI BAO [BEIJING SCIENCE AND TECHNOLOGY NEWS] in Chinese 24 Feb 90 p 3

[Text] The nuclear industry's Institute No 2 for Research and Design (Beijing Institute of Nuclear Engineering) is under the jurisdiction of the China National Nuclear Industry Corporation (formerly the Ministry of Nuclear Industry). The institute was established on 8 January 1958, and is China's largest nuclear research institute. The institute has a total of 2,050 workers, including 1,500 engineering and technical staff and 570 senior engineers. The institute covers more than 60 technical areas including reactor physics, thermal engineering, dosage protection, environmental protection, chemical engineering, waste management, machinery, automation and control instrumentation, graphics, budgeting, water supply, heating and ventilation, electrical, communications, construction, environmental evaluation, and mechanics. Since the start of the institute, more than 400 designs have been put forth and more than 1,160 research topics have been completed. Over the years the institute has received 320 national awards, national science council awards, ministerial merit awards and science and technology achievement awards.

The No 2 Research Institute is responsible for the research and design of production-type nuclear reactor engineering and the reprocessing of nuclear fuel. It has contributed to the establishment of a complete nuclear industry system in China.

After the 3d Plenary Session of the 11th Party Central Committee, the institute adhered to the policy of "making nuclear power the main focus, making a great effort to transfer the technology to the civilian sector, actively developing the nuclear energy industry and trying to diversify," according to the state's reform and openness spirit. Under the guidance of this policy, staff and workers of the institute assumed the responsibility of management and technical services for the Dayawan Nuclear Power Plant in Guangdong, the waste-treatment design of the phase-I engineering of the Qinshan nuclear power plant, the environmental impact evaluation of the national nuclear facilities, the safety evaluation of the two nuclear power plants in Guangdong and Qinshan, the feasibility study of heating by nuclear power, and the general contracting of the phase-II engineering for the Qinshan nuclear power plant.

In the area of isotope applications, the institute has completed the design of large radiation centers (over 500,000 Curies) at Zhengzhou, Nanjing, and Lanzhou, a number of medium and small radiation centers and some special radiation facilities. Radioactive isotopes can be used in the sterilization of wool, leather, and medical equipment; in keeping food, fruits and vegetables fresh; mold prevention of handicrafts and wood and bamboo products; and property modification of plastics and other chemical material. In addition, the institute has also completed the engineering design of gamma-ray measurement facilities at Daqing, Dagang, Huabei, and Yumen.

While perfecting nuclear technology, the institute has also taken on the job of designing various civilian engineering projects. They have designed 70 beer brewers with annual output from 10,000 to 100,000 tons of beer in Beijing, Harbin, Shenyang, and Chongqing, at a combined annual output of about one-third of China's beer production. They have also assumed the task of designing medium and small thermal electric-power plants in Xinjiang, Gansu, Beijing, and Tianjin.

In civilian structures, they have cooperated with the Japanese and designed the China-Japan hospital and the China-Japan Youth Exchange Center, and completed the design of the medium-size guest house and staff residence in the China International Trade Center. They have also designed the Lidu Hotel in Beijing, and the Dunxing building, the Real Estate Company building and the Tongjian Building in Shenzhen.

In recent years, in order to satisfy the needs in science and technology development, the institute has imported from the United States a CYBER 180/830 computer, together with dozens of microcomputer terminals and a CAD design system. The product-design department is equipped with an OCE7500 large-scale automatic drawing-reproduction machine and Chinese and foreign-language computer typewriters.

To meet the needs in the design market, Institute No 2 of the nuclear industry has initiated broad technical cooperation and exchange with foreign countries. From 1986 to May 1989, the institute sent 315 engineers and technicians to 22 countries including the United States, Great Britain, the FRG, Japan, France, and the Soviet Union for visits, training, attendance at international conferences, and for work.

From 1986 to 1988, the institute received 446 groups totaling 5,431 visits from 21 countries including Japan, the United States, France, the FRG, Canada, and Pakistan for academic exchanges and technical cooperation.

The institute is a state-certified design unit authorized to contract design jobs and authorized to accept and train masters-level graduate students. The institute is a Level-I design unit and passed the comprehensive quality management certification in September 1989. Engineers and staff at the institute adhere to their set policy and provide services in engineering design, general contracting or subcontracting, joint development, research, technical consulting, personnel training, equipment manufacturing, and foreign-language translation.

China Moves Into Space Market by Long Marches

[Article by Li Hong]

[Text] Most foreigners, and Chinese citizens, too, think of China as the land of the bicycle.

However, they may have to adjust that image today, if, as scheduled, a U.S.-built communications satellite is launched into space aboard a Chinese Long March-3 rocket booster from a space center set in the hilly woodlands of southern Sichuan Province.

Preparations are said ready to fire the AsiaSat-I into distant geostationary orbit, 36,000 kilometers away from the equator.

If the launch is successful, AsiaSat-I will mark China's entry into the international space market, which will be followed by two more U.S.-made communications satellites to be delivered by China's rockets for the Australian Satellite Company. Further orders for China's series of Long March rockets are expected to come along.

All this will amaze the world.

"Our painstaking research never stopped, even during the 10 tumultuous years of the 'cultural revolution,' and our strength has been built bit by bit," Sun Jiadong, vice-minister of China's space industry as well as a renowned space expert, who led the research and launching of China's first satellite, Dongfanghong-I in 1970, told CHINA DAILY in a recent interview.

The latest statistics show that China has so far successfully launched 26 satellites, with only one failure in 1974. The most recent one, China's fifth telecom-satellite, which was sent into geostationary orbit by a Long March-3 carrier at Xichang launching pad on 4 February this year, served as a dry run for the AsiaSat-I.

To date, China has successfully launched low-orbit return satellites, geo-synchronous orbit telecommunications and broadcasting satellites, and meteorological satellites.

Carriers

As satellites cannot fly without carriers, China has achieved remarkable progress in rocket technology, too, enabling the country to squeeze into the competitive world launching market. Since the 1950s, China has developed various models of the "Long March" rockets, which can launch near-earth orbit satellites, solar-synchronous orbit satellites and geo-synchronous orbit satellites. Twenty of China's 26 satellites were launched by the "Long March" carrier rockets.

The "Long March 1" rocket, which delivered China's first 173-kg satellite "Dongfanghong 1" into space, is able to send a satellite of up to 200 kg into near-earth orbit.

Later, China added two new members to the family of the "Long March" satellites—the reinforced model of the "Long March 2" and the improved model of the "Long March 3," which can carry eight-ton satellites into near-orbit and 2.5-ton satellites to geo-synchronous orbit, respectively.

In December 1988, China used its newly-developed "Long March 4" rocket to launch an experimental weather satellite. The model, a three-stage rocket using conventional liquid fuel, has a lift-off weight of 249 tons, a lift-off thrust of 300 tons, and a payload capacity in solar-synchronous orbit of 2,500 kg.

In addition, China has launching pads in Jiuquan in Gansu Province, Xichang in Sichuan Province and Taiyuan in Shanxi Province. Also, a new launching pad for space research is in the building on Hainan Island, one of the few launching pads near the equator in the world.

Reminiscent of more than 30 years of independent hard research, the vice-minister was a bit exhilarated because all the endeavors he and his colleagues have devoted to their motherland have paid off.

"China is the fifth country in the world to develop and launch man-made satellites independently, the third to be able to retrieve satellites, the fourth to launch multiple satellites with a single rocket, and the fifth to launch geostationary satellites with its own carrier rockets," Sun said.

In December 1957, the Soviet Union, in fierce competition with the United States, launched its Soviet-made "Sputnik 1" satellite into space, the first ever. Since then, China has been determined to launch its own satellite and made it possible by the country's ability to manufacture the carriers of satellites—rockets.

Sophisticated as it is, the launching of a satellite includes four systems: satellite structure, means of delivery, launching sites, and ground control and observation system. In 1967, nearly all the brains related to space research throughout China were rallied in Beijing, declaring the foundation of China's Academy of Space Technology (CAST).

Soon a preliminary scenario was worked out after a series of feasibility studies. China's Academy of Sciences was to manufacture the satellite body and ground sensing project, the then Ministry of Astronautics to make the rocket, and the then Scientific Committee of National Defense was to be responsible to build the satellite launching site.

Disturbed

Later, they named the satellite "Dongfanghong 1" (the East is Red) and planned that its weight should not be less than 150 kg, and that it would be delivered by "the Long March-1" rocket.

The beginning of the "cultural revolution" in 1966 seriously disturbed the satellite program. Owing greatly to Premier Zhou Enlai, who ordered military protection

AEROSPACE

of some key satellite research organizations, most of the scientists were not forced out of their laboratories.

Just as 1 October 1949 will be remembered forever by all the people of China, that of 24 April 1970 is also a landmark in China's history when China's first independently-made satellite, "the East is Red I," was sent into space.

After the Soviet Union, the United States, France and Japan, China was the fifth country to launch its own satellite.

No wonder at all that many Chinese people could not refrain from crying when they heard clearly the melodious music of "the East is Red," transmitted by the first satellite.

"In fact, China's desire and research work toward launching a retrievable satellite walked hand in hand with the 'Dongfanghong 1,'" Sun said.

Then, only the Soviet Union and the United States grasped the technology of launching and recovering satellites, and the latter finally succeeded after experiencing 12 failures.

In 1974, China's first launching of a retrievable satellite failed, too, because a conducting wire of the rocket control system malfunctioned.

But it was just an accident. Since then, all the following 12 recoverable satellites have been successfully launched and retrieved, recording the highest success rate in the world.

China's probe into space never halted. Soon after the launching of its retrievable satellite, scientists started another project to research and develop a geostationary orbit telecommunications satellite.

It succeeded, too. In 1984 an experimental satellite went into orbit and positioned itself there, 36,000 km above the equator. According to Sun, to date China has sent six such satellites into outer space on board the "Long March-3" rockets.

The vice-minister was especially fascinated with China's telecommunications satellite. "Take the one launched in 1986, for example, the strong beam antenna used by the satellite is able to cover all of China with its signals. The launching power of the satellite is the same as that of the International IV and International V, the most advanced telecommunications satellites in the world, but with transmission of clearer television pictures."

Limited by the country's economic strength, China's space industry is not likely to develop on a large scale. Starting in the 1980s, China tended to develop and launch more practical satellites in order to aid its underdeveloped economy.

In September 1988, China's first meteorological satellite "Fengyun (Wind and Cloud) No 1," was sent into 900-km solar-synchronous orbit on the head of a "Long March-4" carrier rocket.

According to Sun, in the days to come, China will give priority to development and launching of satellites greatly needed by the government, particularly satellites for surveys, meteorological observation, telecommunications and broadcasting services, resources investigation and scientific experiments.

Mechanical Properties of ZrO$_2$-Al$_2$O$_3$ Ceramic Composites

40090013a Beijing GUISUAN (AN XUEBAO [JOURNAL OF THE CHINESE CERAMIC SOCIETY] in Chinese Vol 18 No 1, Feb 90 pp 39-46

[English abstract of article by Li Tingkai [2621 1694 0418], Shen Zhijian [3088 1807 1917] et al., of Zhejiang University]

[Text] The mechanical properties of ZrO$_2$-Al$_2$O$_3$ ceramic composites have been studied. It is found that there are two suitable ranges within the ZrO$_2$-Al$_2$O$_3$ system. For ceramics with an Al$_2$O$_3$ matrix, toughening and strengthening of alumina ceramics can be obtained through the addition of ZrO$_2$ grains. For ceramics with a ZrO$_2$ matrix, the strength and fracture toughness of the ZrO$_2$ ceramic can be increased by adding a small amount of α-Al$_2$O$_3$. This is because the crack deflection caused by α-Al$_2$O$_3$ can strengthen the transformation toughening of the ZrO$_2$. By controlling the Y$_2$O$_3$ content in YMSZ [Y$_2$O$_3$ metastable ZrO$_2$] and the Al$_2$O$_3$ content in TZP [Y$_2$O$_3$ metastable ZrO$_2$], ZrO$_2$-Al$_2$O$_3$ ceramic composites with higher toughness and strength can be obtained.

References

1. Li Tingkai, Du Haiqing, JOURNAL OF WUHAN UNIVERSITY OF TECHNOLOGY MATERIALS, No 1, 1988 p 71.

2. Garvie, R.C., et al., J MAT SCI LETTER, No 1, 1982 p 437.

3. Li Tingkai, et al., SCI CERAM, Vol 14, 1988 p 745.

4. Li Tingkai, et al., JOURNAL OF THE CHINESE CERAMIC SOCIETY, Vol 16 No 3, 1988 p 221.

5. Green, D.J., J AMER CERAM SOC, Vol 64 No 3, 1981 p 138.

6. Evans, A.G., "Advances in Ceramics," Vol 12, N. Claussen, et al., ed., 1984, p 193.

7. Li Tingkai, et al., J AUSTRALIA CERAM SOC, Vol 23 No 2, 1988 p 105.

8. Tsukuma, K., Kuniroshi, U., J AMER CERAM SOC, Vol 68 No 1, 1985 p C-4.

9. Wang Youwen, et al., "Proceedings of International Conference on Composite Interfaces-II," H. Ishida, ed., Elsevier Science Publishing Co., Inc., 1988 p 345.

Investigation of Microstructure, Properties of ZrO$_2$-2 mol Percent Y$_2$O$_3$ Ceramics

40090013b Beijing GUISUANYAN XUEBAO [JOURNAL OF THE CHINESE CERAMIC SOCIETY] in Chinese Vol 18 No 1, Feb 90 pp 47-53

[English abstract of article by Ge Qilu [5514 0796 6922], Zhou Yu [0719 3768] et al., of Harbin Institute of Technology]

[Text] The phase content, microstructure, and mechanical properties of zirconia ceramics partially stabilized by yttria (Y-PSZ), and its relationship with the sintering process are investigated by means of X-ray diffraction, SEM and TEM. The samples used were compacted by cold isostatic pressing and sintered at various temperatures. The results show that cold isostatic pressing and the ultra-fine zirconia powder are beneficial for improving the sintering density and microstructure. It is concluded that higher strength and improved toughness can be obtained by mixing tetragonal and suitable monoclinic phases in fine-grain Y-PSZ as well. The Vicker's hardness and fracture toughness of Z$_1$O$_2$-2 mol percent Y$_2$O$_3$ samples sintered at 1600°C for 3 hours followed by slow cooling will be 16.75 GPa and 17.56 MPa x m$^{1/2}$, respectively. The satisfactory hardness and toughness obtained may be considered to result from the combined effect of fine grain size, high density and toughening of microcracks and phase transformation.

References

1. Garvie, R.C., et al., NATURE, Vol 258, 1975 p 703.

2. Murase, Y., Kato, E., J AMER CERAM SOC, Vol 62, 1979 p 528.

3. Sakuma,T., et al., ZIRCONIA CERAMICS, Vol 3, 1985 p 15.

4. Claussen, N., Ruhle, M., ADVANCE IN CERAMICS, Vol 3, 1981 p 137.

5. Ingel, R.P., et al., J AMER CERAM SOC, Vol 65, 1982 p C-150.

6. Rice, R.W., CERAM ENG SCI PROC, Nos 7-8, 1985 p 589.

Effects of ZrO$_2$ Transformation on Strength, Toughness of ZrB$_2$ Ceramics

40090013c Beijing GUISUANYAN XUEBAO [JOURNAL OF THE CHINESE CERAMIC SOCIETY] in Chinese Vol 18 No 1, Feb 90 pp 54-58

[English abstract of article by Zhao Hong [6392 1347], Jin Zongzhe [6855 1350 0772] et al., of the China Building Materials Academy]

[Text] The effects of ZrO$_2$ transformation on the strength and toughness of ZrB$_2$ ceramics are studied based on the mechanical properties and microstructure of ZrB$_2$ ceramics containing 0-30 wt percent of ZrO$_2$.

The strengthening and toughening mechanisms are also discussed by means of several strengthening and toughening models, and by the use of energy-balance theory. The results show that the bending strength and toughness of ZrB_2 ceramics can be increased effectively with the aid of ZrO_2 transformation.

References

1. Tsukuma, K., et al., J AMER CERAM SOC, Vol 68 No 1, 1985 p C-4.

2. Claussen, N., J AMER CERAM SOC, Vol 59 Nos 1-2, 1976 p 49.

3. Sheng Xumin, Xu Jie, JOURNAL OF THE CHINESE CERAMIC SOCIETY, Vol 13 No 3, 1985 p 365.

4. Sheng Xumin, et al., JOURNAL OF THE CHINESE CERAMIC SOCIETY, Vol 14 No 2, 1986 p 153.

5. Qi Mingyuan, et al., J AMER CERAM SOC, Vol 69 No 3, 1986 p 265.

6. Swain, M.V., ACTA METALL, Vol 33, 1985 p 2083.

7. Lange, F.F., J AMER CERAM SOC, Vol 17, 1982 p 225.

8. Evans, A.G., "Fracture in Ceramic Materials," Noges Publications, 1984, p 16.

9. Garrie, R.C., Nicholson, P.S., J AMER CERAM SOC, Vol 55 No 6, 1972 p 303.

Biomembrane, Membrane Bioengineering Studies Reviewed

90CF0226A Beijing KEJI RIBAO [SCIENCE AND TECHNOLOGY DAILY] in Chinese 27 Nov 89 p 2

[Article by Liu Qin [0491 0530]]

[Text] A national priority laboratory on biomembrane and membrane bioengineering established in 1988 is now open to Chinese and foreign scientists. This laboratory was built on the basis of laboratories engaged in biomembrane and bioengineering, including the Zoology Institute of the Chinese Academy of Sciences and the Biological Science and Technology Department of Qinghua University.

Biomembrane and membrane bioengineering is an important direction in modern biological science. It combines modern biology, modern physics, and related engineering disciplines, and is instrumental in the interpretation of biological energy conversion, information recognition and transmission, and mass transfer. It also has potential for practical applications in agriculture and medicine. In the long term it can lead to such emerging technologies as biological transducers, biological separators and concentrators, biological sensors and biological computers. It may serve the national economy and defense in a broad way.

In foreign countries the study of biomembranes began in the 1950's. As a merging of physics, chemistry, biochemistry, and traditional cell biology, membrane engineering and biomembranes gradually formed a new field. In the 1970's this field began to flourish and has now become one of the frontier areas in life science. Many of the fundamental topics in life phenomena, such as biological energy conversion, information recognition and transmission, mass transfer, neurological transmission, hormone regulation, cell immunity, and tumor formation and prevention, are subjects of study in the biomembrane area. Moreover, research on biomembranes is important to other branches of life sciences, including molecular biology, cell biology, neurobiology, growth and senescence study, and oncology. Biomembranes are therefore a merging point for biology, medicine, and agriculture. The technology of artificial membranes, one of the developmental directions in biomembrane engineering, is a promising development in biotechnology. It has had a history of only about 10 years but has already shown unique advantages. It has developed into an independent new biotechnology, especially in the development of the so-called "missile" liposome as an immuno-liposome, and the combination of artificial membranes with gene transduction, cell fusion and immunology engineering.

Biomembrane research at the Institute of Zoology of the Chinese Academy of Sciences is at the cutting edge of the world. Qinghua University has made considerable advances in the study of the structure, phase change, rheology, and other related biological functions of artificial and natural membranes with modern physical methods. The Biology Department of Beijing University has also made important contributions over the years in research on the electro-physiology of excitable membranes. After the scrutiny of experts, this laboratory was listed by the State Planning Commission as a national priority laboratory in 1988 and opened to the outside.

The major research directions of the national biomembrane and membrane bioengineering laboratory are:

(1) Fundamental studies of biomembranes: 1) Structure of biomembranes, 2) Energy conversion through biomembranes, 3) Information identification and transmission, 4) Mechanism for membrane fusion, 5) Research on new mechanisms for the proton pump, 6) Study of artificial membranes and liposomes, 7) Excitable membranes, 8) Cell membranes and environmental toxicity interaction, and cell membrane and cell-skeleton protein interaction.

(2) Application and development of membrane bioengineering: 1) Building of a broad-based biomembrane bioengineering R&D technology, 2) Applications of biomembranes to clinical medicine, 3) Applications of membrane bioengineering in plant genetic engineering, 4) Applications of membrane bioengineering in environmental protection and sanitation.

The policy of the national biomembrane and membrane bioengineering laboratory is "open, dynamic and collaborative." It practices use of the director responsibility system and the academic committee evaluation system. The academic committee is responsible for evaluating the research proposals and the research results and for coordinating the opening of the laboratory to the outside. The current director of the laboratory is Professor Liu Shusen [0491 2885 2773]. Chinese and foreign scientists are welcome to do research here.

The laboratory is equipped with a multichannel cross-correlation fluorophotometer with submicrosecond resolution, an ultra-centrifuge, a flowing-cell spectrophotometer, a photon-counting spectrofluorophotometer, a fast protein liquid chromatograph, a multi-function electrophoresis system, an ultra-thin microtome, a freeze dehydrator, a nuclear-magnetic-resonance spectrometer, a laser microscope, memory oscilloscope, ultraviolet and visible light photometer, a column analyzer and other equipment of the mid-1980's standard.

Artificially Controlled Crop Genetics Developed

90CF0226B Beijing RENMIN RIBAO in Chinese 2 Dec 89 p 1

[Article by Lu Guoyuan [7120 0948 0337]]

[Text] Shanghai, 1 Dec (XINHUA)—The dream of controlling crop genetics by bioengineering technology and creating new species of crops to serve mankind is being realized in China.

Since 1978, the Shanghai Institute of Biochemistry of the Chinese Academy of Sciences, the Institute of Economic Crops of the Jiangsu Academy of Agriculture, and the Crop Hybrid Cultivation Institute of the Chinese Academy of Agriculture have worked together on crop genetics research. After 11 years of exploration, they have developed the first genetic-control technique for crops—the bioengineering technique of introducing DNA from an external source after pollination. DNA (deoxyribonucleic acid) is the large biological molecule that carries genetic information. While conducting repeated tests, scientists have also cultivated new breeds of crops and obtained economically viable breeds of rice cotton. A new breed of cotton, No 3118, has the disease resistance of island cotton (DNA donor) and the high-yield characteristics of mainland cotton (DNA receptor). It has been stably bred to the ninth generation and the yield was 20 to 70 percent higher than that for the receptor. This cotton was planted in 12,000 mu and has increased production by 15 percent or more. A new breed of rice, No 829042, obtained by introducing the DNA of early mature purple corn has desirable features of drought resistance and early maturing. It is being tested in dry fields near Beijing. By introducing into rice external DNA of tare, kaoliang, and purple rice, special breeds and offspring with donor properties have been obtained.

The molecular breeding technology invented by the Chinese has attracted attention in the international scientific community.

According to experts here, the emergence of the new bioengineering technology for introducing external DNA after pollination not only has provided a good experimental system for studying the introduction of external DNA, but also has broadened the scope for plant variation. In crop breeding, this is a valuable new avenue. Its advantages include the simplicity of the method, the modest equipment requirement, and its general applicability.

First Gene-Engineered Transgenic Animals Produced

90CF0226C Beijing RENMIN RIBAO in Chinese 8 Dec 89 p 2

[Article by Zhao Xiaomei [6392 2556 2734] and Zhang Xuechuan [1728 1331 0356]]

[Text] Shanghai, 6 Dec (XINHUA)—A major breakthrough has been achieved in China's animal genetic engineering research. Using genetic engineering technology, scientists have obtained the first batch of transgenic rabbits by injecting genes containing hepatitis B virus and human growth hormone into the fertilized eggs of domesticated rabbits.

This success has broken the barrier that prevented most animals from hybridization. It is highly significant for species improvement by using desirable genes of other species.

When the scientists first researched transgenic rabbits, they used microinjection to introduce the surface antigen of the hepatitis B virus into the male procaryon of a fertilized egg of a rabbit. They then transferred it to the oviduct and into the uterus of a female rabbit, until the rabbit gave birth to a transgenic rabbit. After tests of molecular hybridization and immuno-enzyme marking, the surface antigen of hepatitis B and its products were found in the blood of the transgenic rabbit and its offspring. This indicates that the external gene has existed, exhibited and propagated in the genes of the transgenic rabbit.

Computer Viruses Threaten Networks

40100043a Beijing CHINA DAILY in English
18 Apr 90 p 3

[Text] Chinese officials from a computer virus monitoring center under the Ministry of Public Security have confirmed that many of the country's computers were afflicted by widespread virus named Jerusalem last Friday.

As viruses spread through China's computers, experts are urging measures to protect these vital networks.

Thousands of computers have already been infected by the external virus, according to the Beijing-based SCIENCE AND TECHNOLOGY DAILY.

A sample survey conducted in Beijing found that hundreds of the city's computers have been affected by six viruses: Jerusalem, Vienna, Brain, 648, Hemp, and Yankee-doodle.

The infection is on the increase, the paper reported.

This threatens computer data bases which could result in severe losses.

The regular work of a computer center in one of the capital's universities was suspended because all the center's 50 terminals were infected by the virus within a week, the paper said.

Normal production at a Beijing chemical factory was slowed for a month when the virus attacked company computers.

The six viruses found in Beijing afflict computers by lowering their functions, damaging their normal programs or deleting all their stored information.

Officials are urging a complete check of China's computers and disks.

Safeguards must be taken by all users to verify, segregate and eliminate a computer virus as soon as they find one. These findings should then be reported to local public security sections without delay.

First Domestic "Tempest"-Protected Computer Developed

90P60002a Beijing KEJI RIBAO [SCIENCE AND TECHNOLOGY DAILY] in Chinese 27 Mar 90 p 2

[Article by Wang Hanlin [3769 5060 2651]: "Institute 706 of Ministry of Aeronautics and Astronautics Industry Achieves Breakthrough: Development of China's First Anti-Information-Leak Computer," based on report by Sun Minqiang [1327 3046 1730] in ZHONGGUO HANGKONG HANGTIAN BAO]

[Summary] China has made a breakthrough advance in countering information leaks from computers—a technology tightly restricted abroad and highly competitive. Trials of the anti-information-leak computer developed by Institute 706 of the Ministry of Aeronautics and Astronautics Industry (MAAI) have generated satisfying results.

Since a great amount of military, political and economic information escapes through electromagnetic emanations from computers, it is susceptible to theft by resourceful individuals with advanced receiving and processing equipment. As an example, this writer recently witnessed a demonstration in which a common TV set, with some modifications, was able to display the complete contents of a computer monitor positioned several dozen meters away.

The mysterious anti-information-leak technology known abroad as "Tempest" has been tightly guarded by foreign nations and has also been the subject of intensely competitive development projects. On its own initiative, and with no technical reference data, MAAI's Institute 706 boldly undertook the difficult task of developing such a system. Using both offensive and defensive tactics in a two-year-plus research effort, the institute finally developed China's first anti-information-leak computer. Tested by various authorities, this equipment has performed well.

Advances in Speech Recognition

Shanghai Computing Institute's System Reported

90P60001a Beijing JISUANJI SHIJIE [CHINA COMPUTERWORLD] in Chinese No 7,
21 Feb 90 p 20

[Article by Wang Zhengsan [3769 2973 0005]: "Shanghai Institute of Computing Markets Restricted Chinese-Character-Set Mandarin Speech-Recognition System"]

[Summary] The "restricted Chinese-character-set Mandarin speech-recognition system" developed in a one-year-plus effort by the Shanghai Institute of Computing recently passed its technical appraisal. The system, which runs on an IBM PC/XT or compatible, is designed to distinguish homonyms and near-homonyms. In specific technical areas (currently restricted to weather forecasting), the system can perform statistical analyses of original data input via spoken commands and in complete spoken sentences, and can automatically transliterate all of its Chinese data files into Pinyin.

The system includes the U.S.-made "Voice Command" plug-in speech card, a microphone, CCDOS [Chinese-character DOS] version 2.1 or higher, and one LCRS system disk. Tested with 36 days' worth of 1986 Shanghai weather forecasts (3 days from each month)—76,589 total characters, 182 different characters, and 64 high-frequency compounds or word groups, all requiring 16 minutes for statistical scanning—the system demonstrated an accuracy of 88.9 percent for recognizing the compounds. With one or two repetitions of the sound, accuracy approaches 100 percent.

Sida 252 System Released

[Article by Liu [0491]: "Sida 252 Chinese-Character
Speech System Debuts"]

[Summary] The Sida [0934 6671] 252 Chinese-
character speech system, which uses monosyllables as
the units to be recognized, recently made its debut.
Advanced algorithms are used for the digital pro-
cessing of speech signals in this real-time speech-
recognition system, which employs the TMS320C25
high-speed signal-acquisition, processing and synthesis
board. All Chinese characters in the GB1- and GB2-
level character sets may be input.

Tested over a long period, the system's recognition rate
for Mandarin Chinese averaged 89.1 percent, with the
rate for the first two speakers tested reaching as high as
98.0 percent. The system response time is 0.2 second,
and over 30 characters can be input per minute. To a
certain extent, local accents of Mandarin can be correctly
recognized by the system. Experts at the recent technical
accreditation sponsored by the Beijing Municipal Sci-
ence and Technology Commission and the Municipal
People's Government commented that the Sida 252
system is the best among full-syllable Chinese speech-
recognition systems, and that its speech-synthesis tech-
nology has reached the world-class level.

Project Planned to Build Robots

[Text] China has begun the development of five types of intelligent robots and plans to form a robot production industry by 1995. This was disclosed at a working conference on robots in Shenyang on Friday [23 March 1990].

The five types include intelligent assembly robots, cableless underwater robots, movable program-controlled robots for operations in adverse environments, antinuclear and antichemical reconnaissance robots, and wall-crawling inspection robots.

The development of intelligent robots is listed as China's High Technology Research Plan No 863. The program will be carried out by the Robot Engineering Center of the Shenyang Automation Institute, Chinese Academy of Sciences, and other scientific research units in China's major universities and colleges.

New Laser Excitation Process for Uranium Isotope Separation

[Article by Xu Baoyu [1776 5508 5940] of the Department of Nuclear Science, Fudan University, Shanghai: "Uranium Isotope Separation Using a Three-Consecutive-Step Resonance Laser Excitation Process"]

[Text] Key words: laser separation of uranium isotopes, non-linear excitation.

Laser separation of uranium isotopes is an important research area that may have large-scale industrial applications in the near future. Several laser uranium isotope separation methods have been investigated, including AVLIS (atomic vapor laser isotope separation),[1] which involves the photo-ionization of urnaium-atom vapor, and MLIS (molecular laser isotope separation),[2] which involves the molecular dissociation of uranium hexafluoride. These methods, in reality, require a multi-step excitation process. However, the effect of the selective excitation of the laser is limited to the first excitation step; other excitation steps do not contribute to the selectivity of the entire process. The only effect is to provide sufficient energy to further ionize or dissociate the excited atom or molecule. Hence, the selectivity of these processes is somewhat limited.

I. Electron Vibration Spectrum and Photochemical Reaction of Uranyl Formate

Some uranyl compounds have narrow absorption bands at low temperatures. Hence, they have distinct electron vibration structures and the isotope shift is noticeable,[3] as shown in Figure 1. In the figure, v_a and v_a' represent the asymmetric-elongation vibration mode in the ground and first electron excitation states, respectively. Based on available spectral data,[4,5] the isotope shifts and absorption bandwidths of various energy-level transitions for single-crystal liquid uranyl formate are:

$$\Delta v_1 \simeq 1.05 - 0.35 = 0.70 cm^{-1}; \quad [FWHM]_1 \simeq 7.5 cm^{-1};$$

$$\Delta v_2 \simeq 1.05 - 0.25 = 0.80 cm^{-1}; \quad [FWHM]_2 \simeq 0.81 cm^{-1};$$

$$\Delta v_3 \simeq 1.25 - 0.25 = 1.0 cm^{-1}; \quad [FWHM]_3 \simeq 7.5 cm^{-1}.$$
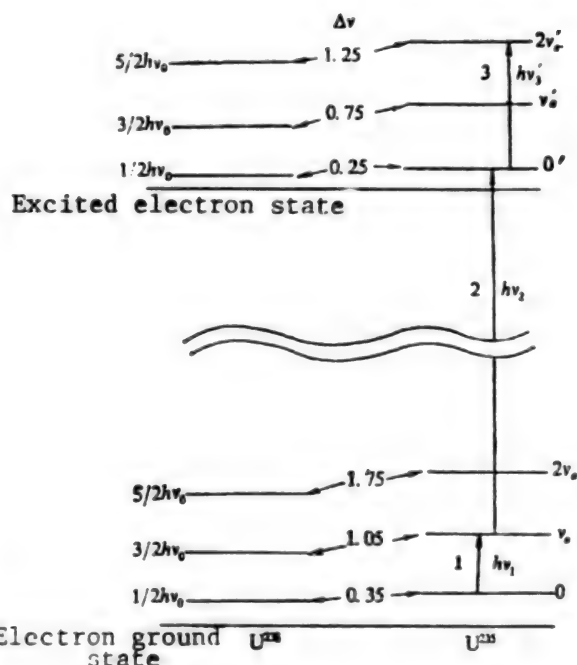

Figure 1. Electron Vibration Absorption Spectrum of Single-Crystal Liquid Uranyl Formate

Photochemical reactions of solid uranyl-formate compounds in visible and ultraviolet light and their photo-dissociation by resonance with an infrared laser have been studied.[6,7] Figure 2 shows the internal energy levels and reaction coordinate of the molecule. Thus, by using three laser frequencies, which match the three continuous steps of absorption frequencies at the U^{235} isotope molecule, one can excite this molecule all the way to the second vibrational excitation state in the first electon excitation level. A single-crystal liquid uranyl-formate molecule in this high energy state can undergo photochemical reactions to form lower-valence uranium oxides due to the reductive nature of the formate ion. The lower-valence uranium oxides enriched with U^{235} can be easily separated from U^{238} uranyl-formate molecules that have not been excited and have not undergone photochemical reactions using an anion-exchange resin.[8]
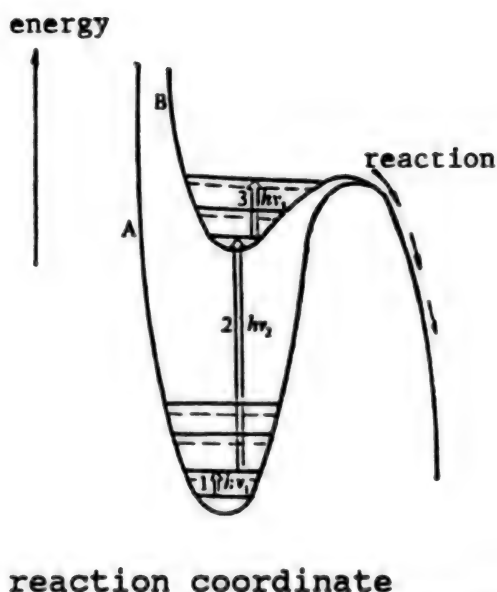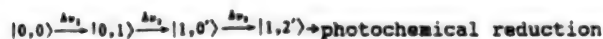
energy

reaction coordinate

Figure 2. Potential-Energy Curve of Single-Crystal Liquid Uranyl-Formate Molecule and the Photochemical Reaction

From Figure 2 we know that the three consecutive transition steps involve the following energy levels:

$$|0,0) \xrightarrow{\Delta\nu_1} |0,1) \xrightarrow{\Delta\nu_2} |1,0') \xrightarrow{\Delta\nu_3} |1,2') \rightarrow \text{photochemical reduction}$$

where the numbers in each bracket represent the quantum numbers of the electron state and vibrational state, respectively. The " ' " mark indicates that the number is a vibrational quantum number of an excited state. Based on the available infrared absorption spectrum[4] and fluorescence excitation spectrum[5] of single-crystal liquid uranyl formate, the absorption frequency range of the first excitation step is 933 cm^{-1}, which is equal to ν_a. The second step corresponds to 19660 cm^{-1}, which is equal to the difference between the fluorescence resonance frequency (i.e. 20593 cm^{-1}) and ν_a (i.e. 933 cm^{-1}). The third step corresponds to 1404 cm^{-1}, which is equal to $2\nu_a'$. They are located within the emission frequency ranges of a CO_2 laser, dye laser and CO laser, respectively. As for the fine tuning of each excitation frequency, it is determined by the spectra obtained at the temperature of the separation experiment.

II. Selectivity of the Three-Consecutive-Step Resonance Excitation Process

Because every laser-induced excitation in this non-linear excitation process is rigorously in resonance with the transition between the corresponding energy levels in the

molecule, the overall selectivity S of the entire excitation process is the product of the selectivity of every individual step S_i:[9]

$$S = \prod_i S_i = S_1 \times S_2 \times S_3.$$

The selectivity of every individual step (which is dependent upon its spectral characteristics) is determined by the full width half maximum (FWHM) of the corresponding absorption band and the isotope shift ($\Delta\nu$). It can be expressed as follows:[10]

$$S_i = \left[1 - \frac{\Delta\nu_i}{[\text{FWHM}]_i} \right]^{-1}.$$

Based on the values of $\Delta\nu_i$ and $[(\text{FWHM})]_i$ listed in the previous section, selectivities of all the steps, S_1, S_2, and S_3, can be calculated:

$$S_1 = 1.11, S_2 = 81.0, S_3 = 1.15$$

Hence, the overall selectivity is:

$$S_s = 1.11 \times 81.0 \times 1.15 = 103.$$

The subscript s indicates that it is dependent upon its spectral characteristics in order to differentiate it from the dynamics-related selectivity to be discussed later. Thus, we can see that this three-consecutive-step resonance excitation process has a very high selectivity. This new laser separation technique, theoretically, can enrich natural uranium, which contains 0.72 percent U^{235}, to uranium with a concentration of 74 percent U^{235} in one process.

In reality, in addition to spectral characteristics, the selectivity of this unimolecular photochemical reaction is also determined by the rates K_A and K_B at which these isotopes (denoted as A and B) undergo this photochemical reaction, the rate K_{V-V} at which the vibrational energy between isotope molecules V-V is transferred, and the thermal excitation rate K_T. The dependence of selectivity upon these dynamic characteristics can be expressed as:

$$S_K = K_A(K_B + K_{V-V} + K_T)^{-1}$$

In general, the energy transfer rate between isotope atoms or molecules due to resonance as a result of collision is very fast. However, the relative position between atoms (or ions) is fixed in a crystal. Especially when they are isolated in a matrix, isotope atoms (or

ions) are separated by a large number of other atoms in order to avoid collision. If uranyl formate crystal doped with a high level of other transparent materials is used as the starting material, the K_{V-V} of the excited uranium isotope molecules becomes very negligibly small. In addition, since the coupling between the uranyl ion and the lattice is very weak, the rate of radiationless transition between the electron excitation state and ground state is slow. This radiationless transition is the major source of heat in the system. Therefore, its thermal excitation rate is also small. Finally, since unexcited U^{238} molecules cannot take part in the photochemical reaction at low temperature, i.e. K_B is very small, the excited U^{235} molecule's photochemical reaction rate $K_A >> K_B$. Hence, the process has a high dynamic selectivity S_K. The selectivity of this three-consecutive-step resonance excitation process is ultimately determined by its spectral selectivity and it is expressed as S_s.

III. Conclusion

In summary, the three-consecutive-step resonance laser excitation process presented in this paper is a new type of laser uranium-isotope separation. In principle, it has a higher selectivity than existing laser isotope separation techniques. Experimentally, the selectivty of the first resonance excitation step has been determined and it has been found to be as high as 1.1. This is in agreement with the calculated value S_1. We are in the process of measuring the selectivity of the second and third steps, as well as the overall selectivity of the entire process.

References

1. Davis, J.I., LASER FOCUS, 18, 49, 1982.

2. Horsley, J.A., et al., IEEE J., QE-16, 412, 1980.

3. Rabinowitch, E.I., et al., "Spectroscopy and Photochemistry of Uranyl Compounds", MacMillan, New York, 1-15, 1964.

4. Xu Baoyu, et al., KEXUE TONGBAO, Vol 31, No 15, 1145, 1986.

5. West, W.P., et al., J. CHEM. PHYS., 78, Part 1, 3338, 1983.

6. Claudel, B., et al., JOURNAL OF PHOTOCHEMISTRY, 7, 113, 1977.

7. Xu Baoyu, et al., HUAXUE XUEBAO [ACTA CHIMICA SINICA], 45, 1005, 1987.

8. Kraus, K.A., et al., JACS, 78, 2692, 1956.

9. Letokhov, V.S., "Nonlinear Laser Chemistry", Springer-Verlag, Berlin, Heidelberg, New York, 68-70, 1983.

10. Xu Baoyu, ZHONGGUO JIGUANG [CHINESE JOURNAL OF LASERS], 10, 354, 1983.

Conformal Slot Array Antenna on Large Conducting Cylinder Covered by Dielectric Layer

[Article by Zheng Jingliang [6774 0079 0081], and Yang Qiji [2799 2757 4014] of Qinghua University]

[Text] Abstract: This article discusses the analysis and design methods for a conformal slot-array antenna on a large conducting cylinder covered by a dielectric layer. The moment method is applied to solve the integral equations of the electric fields tangential to the slot surface. The concept of a quasi-symmetric array, which reduces the order of the linear equations by half, is introduced. The equivalent network parameters and directivity patterns are derived for both single-slot elements and the slot array. The amplitude and resonance characteristics of the slot are discussed, and synthetic design methods and procedures for the array are presented. Computer-aided analysis and design methods have been implemented, and the calculated results have been partially verified by experiments.

I. Introduction

The conformal slot-array antenna on a large conducting cylinder covered by a dielectric layer potentially has a wide range of applications in modern aircraft. In this type of antenna, the coupling effect between the elements is enhanced by the dielectric layer; if a rectangular waveguide feed is placed along the axis of the cylinder, the elements can be coupled either through the space outside the cylinder or through the space inside the waveguide. However, in the space outside the cylinder, the equations become more complicated and analysis more difficult due to the increased interface area; the directivity pattern of the cylindrical array cannot be resolved into a product of the pattern for the elements and an array factor, and the unique characteristics of the cylindrical array must be taken into consideration in the analysis and design. The dielectric layer covering the cylinder changes the directivity of the elements, and increases the amplitude of the crawling waves, which in turn raises the level of the diffraction field in the shadow region. These considerations pose new problems for the analysis and design of this type of antenna.

Several studies of the topic of a conformal slot-array antenna on a cylinder covered with a dielectric layer have appeared in the literature. In Ref. [1], [2], the axial magnetic point source and the fields of axial slots are investigated; the convergence properties of the field of axial slots are investigated; the convergence properties of the field equations and methods of improving the convergence are discussed. In Ref. [3], an experimental study of a circumferential slot-array without considering the coupling effects between the elements is reported. In Ref. [4], [5], the calculation of coupling coefficients between slots is discussed. In this article, the analysis of the slot array is extended by taking into account the coupling

LASERS, SENSORS, OPTICS

effects between elements; specifically, the directivity pattern, equivalent network, amplitude and resonance characteristics of single elements and the slot array are discussed. In addition, methods and procedures for synthetic design of slot arrays are investigated, and experimental measurements are made to partially verify these results.

II. Analysis of Slot Array

Consider an array of M_o axial slots on a conducting cylinder covered with a dielectric medium (with dielectric constant ε_1). Assume that it is fed by several waveguides filled with dielectric material (with dielectric constant ε_2) and located inside the cylinder along the cylinder axis; the slots are located on the wider side of the waveguide (Fig. 1). Let the width, length, and the coordinates of the midpoint of the mth slot be denoted by w_m, l_m, and (φ_m, Z_m).
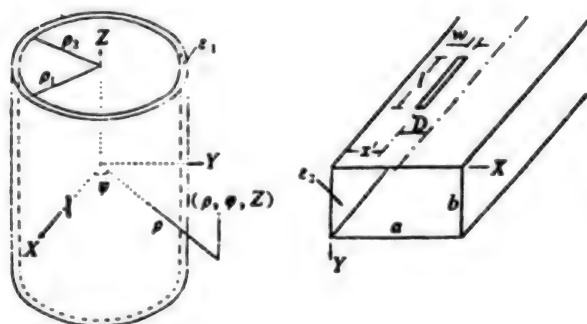

Figure 1. Geometry of Slot Array

The magnetic fields inside and outside the waveguide are expressed in terms of the tangential electric fields at the slot opening so that the two are continuous at the slot surface. One can derive integral equations for the electric fields and solve the linearized equations using the moment method. For an axial slot array, the basis vector function unordered set: $f_{m/p}$ and the test vector function Unordered set: $g_{m/p}$ can be assumed to have only axial components.

$$f_p(\varphi, z) = g_p(\varphi, z) =$$

$$\sqrt{\frac{2}{l_m w_m}} \sin\left(p\pi\left(\frac{1}{2} - \frac{z - z_m}{l_m}\right)\right)\hat{z} \quad (\varphi, z) \in S_m \quad (1)$$

Depending on the end conditions of the feed waveguide, the slot will be excited by either a traveling wave or a standing wave in the waveguide; the corresponding

linear equations when the thickness of the waveguide can be ignored are of the form:

$$\sum_{q=1}^{\infty} \sum_{n=1}^{M_0} \left(Y^{aa}_{\substack{mn \\ pq}} + Y^{bb}_{\substack{mn \\ pq}} \right) J_q = H^i_p$$

(traveling-wave excitation)

$$\sum_{q=1}^{\infty} \sum_{n=1}^{M_0} \left(Y^{cc}_{\substack{mn \\ pq}} + Y^{bb}_{\substack{mn \\ pq}} - Y^{bb}_{\substack{mn \\ pq}} \right) J_q = H^{i,r}_r$$

$$(p = 1, 2, \cdots\cdots \quad m = 1, 2, \cdots M_0)$$

(standing-wave excitation)

$$\tag{2}$$

The unknowns $J_{n/q}$ are the coefficients of expansion of the surface magnetic flux $J^{(m)}_n$ at the slot S_n. $J_{n/q}$ represents the amplitude of the qth mode of the surface magnetic flux.

$$J^{(m)}_n(\varphi, z) = \sum_{q=1}^{\infty} f_q(\varphi, z) J_q \tag{3}$$

The excitation terms $H'_{m/p}$, $H^{i/r}_{m/p}$ on the right side of equation (2) are the contributions of the excitation fields inside the waveguide to the p-mode of the tangential magnetic field at the slot S_m. The coefficients Yaa/mn/pq, Ybb/mn/pq are respectively the mode-coupling coefficients of the slot through the space outside the cylinder and through the space inside the waveguide; in physical terms, they can be interpreted as the contribution of the q-mode surface magnetic flux at the slot S_n to the p-mode tangential magnetic field at the slot S_m. Y/bb/mn/pq, is the mode-coupling coefficient between the image slot $S_{n'}$ of the slot S_n inside the wave-guide and the slot S_m. To calculate the mode-coupling coefficient Y/aa/mn/pq will involve the vector Green's function for the space outside the cylinder. Because of the dielectric layer, these equations become very complicated[1], and have poor convergence properties. In Ref. [2] and Ref. [4], the convergence properties of the series and integral solutions and methods of improving the convergence are investigated by carrying out lengthy mathematical analyses based on expansions of Green's function in terms of its characteristic functions; formulas for numerical computation of the near-field pattern and the coupling coefficients are also derived. To avoid the singularity of the point source of Green's function inside the

waveguide, Ref. [5] has introduced a concept of a gener-alized solution and obtained the mode-coupling coeffi-cient of the slot through the space inside the waveguide, Y/bb/mn/pq.

As far as the feed waveguide is concerned, the slot on the waveguide wall can be regarded as an equivalent T-type network, as shown in Figure 2. The magnitudes of the impedances Z and the admittance Y can be obtained from the following expressions (let the characteristic impedance and characteristic admittance of the trans-mission line be denoted by R_o and G_o respectively):

$$\frac{Z}{R_0} = \frac{C_1}{2-C_1}, \qquad \frac{Y}{G_0} = \frac{-(2-C_1)C_2}{2-C_1+C_2} \qquad (4)$$

$$C_1 = \frac{2}{\omega\mu_0 ab\beta}\left(\frac{\pi}{a}\right)^2 \frac{1}{H_s^2} e^{i2\beta x} \sum_{\substack{p=1 \\ (p\ even)}}^{\infty} H_{\overline{p}}^{i} J_{\overline{p}}$$

$$C_2 = \frac{2}{\omega\mu_0 ab\beta}\left(\frac{\pi}{a}\right)^2 \frac{1}{H_s^2} e^{i2\beta x} \sum_{\substack{p=1 \\ (p\ odd)}}^{\infty} H_{\overline{p}}^{i} J_{\overline{p}} \quad (5)$$
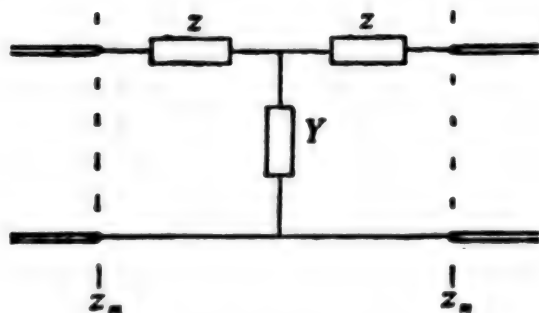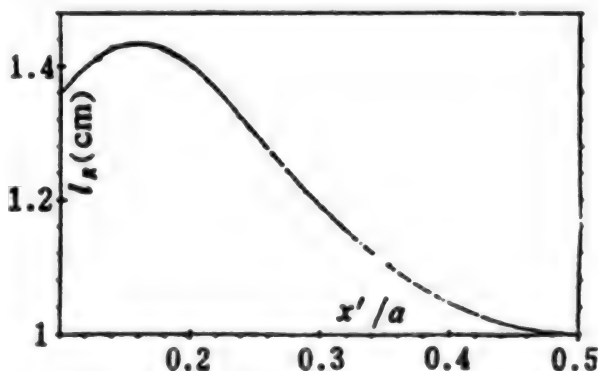

Figure 2. Equivalent T Network

Figure 3. Relationship Between the Resonant Slot Length l_R and Offset Distance D (D/a = 0.5 - x'/a)

When a short circuit exists at the end of the feed waveguide, the reflection coefficient of the waveguide is:

$$\Gamma_s = e^{i2\beta z_{1s}}\left\{-e^{-i2\beta z_{0s}} + \frac{1}{\omega\mu_0 ab\beta}\left(\frac{\pi}{a}\right)^2 \right.$$

$$\left. \frac{1}{H_s^2} \sum_{m \atop (s)} \sum_{p=1}^{\infty} H_{\overline{p}}^{i\ r} J_{\overline{p}}\right\} \qquad (6)$$

where Z_{os}, Z_{1s} are respectively the locations of the short circuit and the reference plane, $\Sigma_{m/(s)}$ denotes the sum-mation with respect to the slots on the sth waveguide, and H_s is the amplitude coefficient of the incident wave inside this waveguide.

Several slots on the same waveguide constitute an axial slot array. In an array surface made of a number of slot arrays, if the slots on symmetrically placed waveguides are not identical, then the array is not symmetrical (see Fig. 8). But if the offset distances of the slots are small, then the coupling coefficients between the slots are almost the same; in other words, when the slot pairs S_{m1} and S_{m2}, S_{n1} and S_{n2} are placed symmetrically, then,

$$Y_{\substack{m_1 n_1 \\ pq}}^{aa} \approx Y_{\substack{m_2 n_2 \\ pq}}^{aa} \qquad Y_{\substack{m_1 n_1 \\ pq}}^{bb} = Y_{\substack{m_2 n_2 \\ pq}}^{bb} \qquad (7)$$

If these differences are neglected, then the order of the equations (2) can be reduced by one half. Such arrays are called quasi-symmetric arrays. If this array is subject to symmetric excitation, then one can obtain a symmetric distribution of the amplitude of the array elements.

The far-field directivity function of the slot elements can be derived:

$$F_s(\theta, \phi) = \Phi(\theta, \phi) \frac{\cos\left(\frac{l}{2}k_0\cos\theta\right)}{\left(\frac{\pi}{l}\right)^2 - (k_0\cos\theta)^2} \qquad (8)$$

Adopting the notations A_o and A_1 from Refs. [2] and [4], the function $\Phi(\theta, \phi)$ in this equation can be expressed as follows (N_n is the Neumann number):

$$\Phi(\theta, \phi) = \frac{1}{2}\left\{\sum_{n=0}^{\infty} N_n j^n \cos(n\phi)\right.$$

$$\left.\frac{A_1}{A_0} \frac{1}{H_n^{(2)}(\sqrt{k_0^2 - u^2\rho_1})}\right\}_{u = k_0\cos\theta} \qquad (9)$$

The directivity function for a T_o-element axial array (where D_i and z_i are respectively the amplitude factor and position coordinate of the array elements) is:

$$F_{az}(\theta, \phi) = F_r(\theta, \phi) F_1(\theta) \qquad (10)$$

$$F_1(\theta) = \sum_{i=1}^{T_0} D_i e^{j k_0 (\cos \theta) z_i} \qquad (11)$$

The directivity function for an S_o-element circumferential array (where B_s, φ_s are respectively the amplitude factor and position coordinate of the array elements) is:

$$F_{a\phi}(\theta, \phi) = \frac{\cos\left(\frac{l}{2} k_0 \cos\theta\right)}{\left(\frac{\pi}{l}\right)^2 - (k_0 \cos\theta)^2} \sum_{s=1}^{S_0} B_s \phi(\theta, \phi - \psi_s) \qquad (12)$$

The directivity function for a surface array is

$$F_a(\theta, \varphi) = F_{a\varphi}(\theta, \varphi) F_1(\theta) \qquad (13)$$

III. Design of Slot Array

Both theoretical analysis and numerical results indicate that for practical slot lengths, the amplitude of the fundamental mode of slot equivalent surface magnetic flux is an order of magnitude higher than the amplitude

of other modes[6]. If the mode-coupling coefficients also satisfy the condition:

$$I_m \left(Y^{aa}_{\substack{mm \\ 11}} + Y^{bb}_{\substack{mm \\ 11}} \right) = 0 \qquad (14)$$

then resonance will occur in the fundamental mode of the surface magnetic flux. In this case, the slot can be regarded as an electric conductor connected in parallel. Fig. 3 shows the relationship between the resonant slot length l_R and the offset distance D of the slot inside the feed waveguide. Figures 4 and 5 show the relationship between several modes of the surface magnetic flux along the resonance slot and the offset distance, and the relationship between the equivalent T-network parameters and the offset distance, respectively. It is seen that by varying the offset distance of the slots in the array, one can adjust the amplitude distribution of the array elements and obtain a matched-feed network. The parameter values for the figure are as follows:

$$\begin{aligned}
&\rho_3 = 0.310m, \quad \rho_1 = 0.312m, \quad f = 9.6GHz \\
&\varepsilon_1 = 2.55\varepsilon_0, \quad \varepsilon_2 = 2.55\varepsilon_0 \\
&a = 15mm, \quad b = 5mm \\
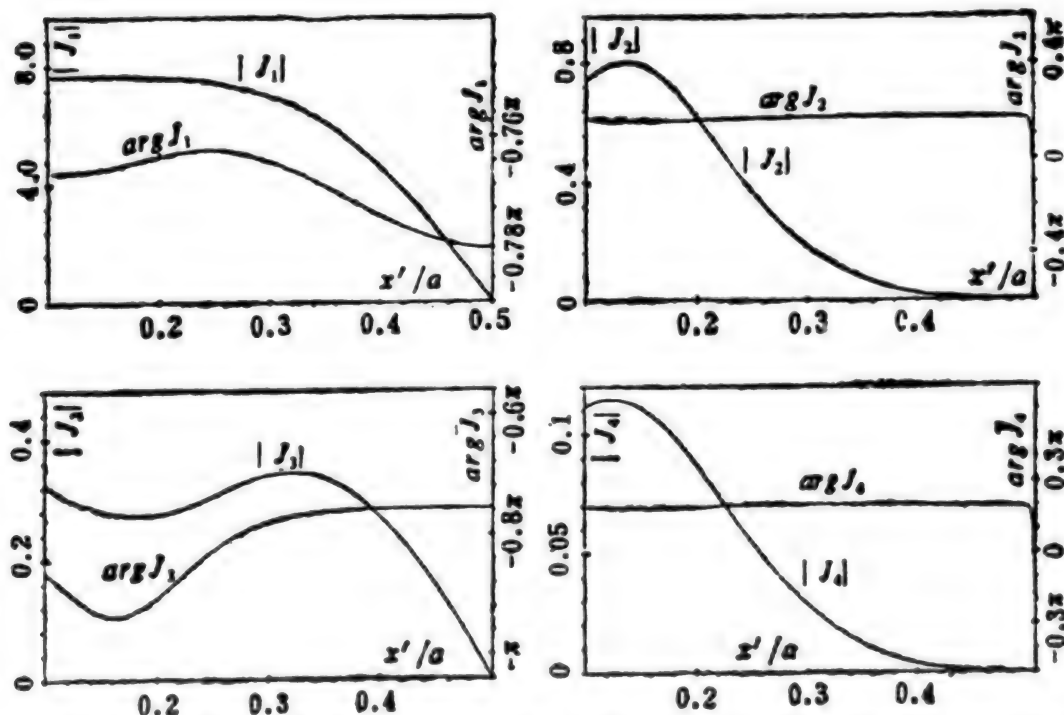&w = 0.77mm, \quad H_s = 1
\end{aligned} \qquad (15)$$

Figure 4. Relationship Between the Different Modes of the Surface Magnetic Flux and the Offset Distance D When Fundamental-Mode Resonance is Due to Standing-Wave Excitation (Distance between the short-circuit plane and the center of the slot is $5/4 \lambda_{7g}$)
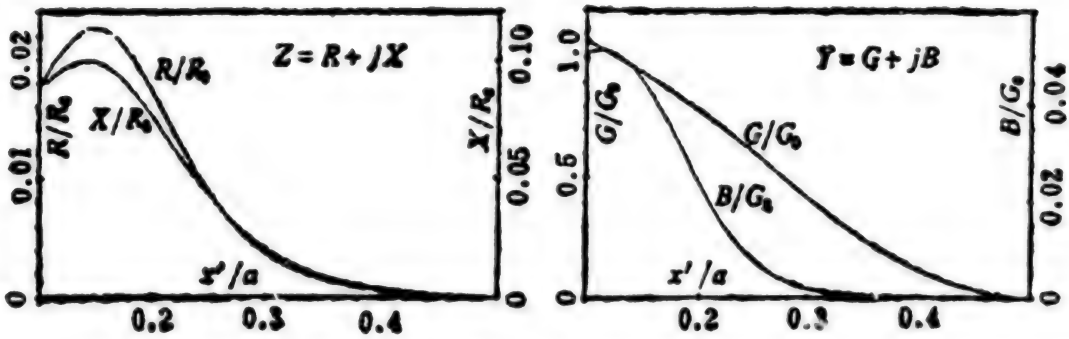
Figure 5. Relationship Between the Parameters of the T-Type Equivalent Network and the Offset Distance D When Resonance Occurs in the Fundamental Mode of the Surface Magnetic Flux (D/a = 0.5 - x'/a)

Comparing equations (10) and (12) shows that the directivity function of the circumferential array $F_{a\varphi}$, unlike that of the axial array F_{az}, cannot be resolved into a product of the element directivity and array directivity. This makes controlling the circumferential directivity of the array very difficult. Since the subtended angle of an array on a cylinder radiating in a fixed direction is generally quite small, the cylindrical surface array can initially be regarded as a planar array tangent to the cylinder, for which the amplitude factor B'_s, of each element can be determined based on the far-field directivity requirement; then the phase of each element is adjusted by an amount which exactly compensates for the phase shift caused by the ray path difference due to the cylindrical surface. Thus, the main lobe and the near-field sidelobes of the circumferential directivity pattern of the cylindrical array are similar to those of the planar array. By substituting the initial B_s into equation (12), the circumferential directivity pattern can be computed and compared with the required pattern; the

difference between the two is used to adjust the value of B_s until a satisfactory pattern is obtained. Figure 6 shows the single-element directivity pattern. The fluctuations in the shadow region are caused by the mutual interference between the diffraction fields crawling along the two sides of the cylinder; the dielectric layer increases the amplitude of the crawling wave and significantly raises the level of the diffraction field in the shadow region. Figure 7 shows the circumferential directivity pattern of a 10-element array designed using the proposed method; the parameter values for this pattern are identical to those given in equation (15). As a result of phase compensation, the phase of the elements in the array advances from the center toward the two sides. If the element spacing is close to the wavelength, the crawling waves will superimpose on one another and produce a high-level diffraction field in the shadow region and in the transition region (e.g., Fig. 7(a)). In this case, the circumferential spacing between the elements must be reduced to avoid super-position of the crawling waves (e.g., Fig. 7(b)).
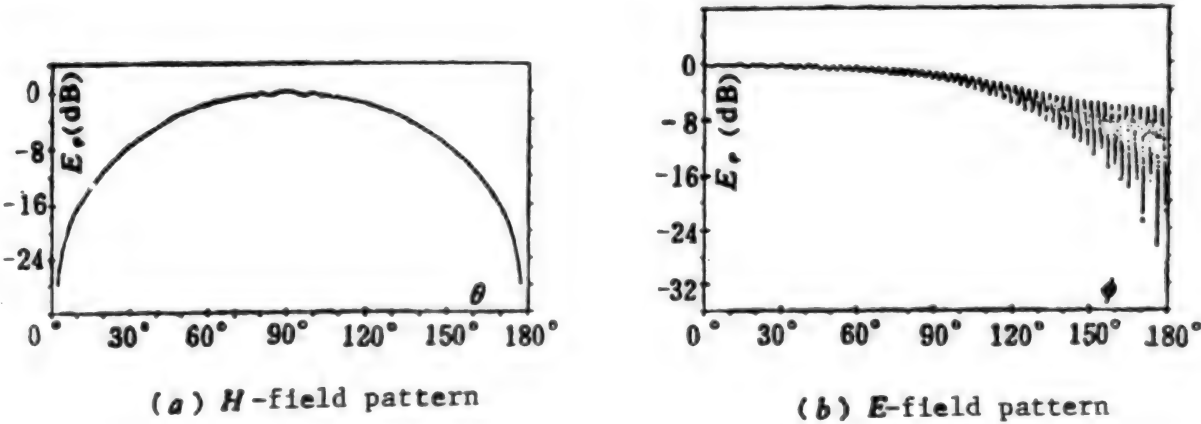

(a) H-field pattern

(b) E-field pattern

Figure 6. Directivity Pattern of Single Element

$$(a) \, \phi_{m+1} - \phi_{p} = 0.02637\pi$$

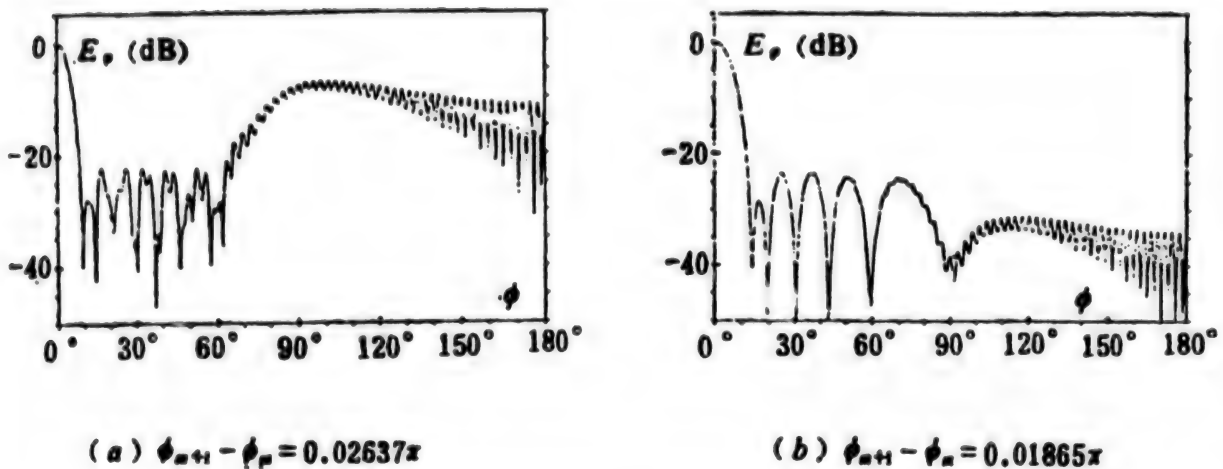$$(b) \, \phi_{m+1} - \phi_{m} = 0.01865\pi$$

Figure 7. E-Field Directivity Pattern of a 10-Element Circumferential Array

The design procedure for the slot array is as follows:

1. Determine the amplitude and phase distribution of the array elements according to the far-field directivity requirement;

2. Carry out preliminary design of the array based on the amplitude and impedance characteristics of the elements;

3. Based on an analysis of the preliminary design, determine the actual array parameters by taking into account coupling effects between the elements;

4. Compare the array parameters with the requirements and examine the differences between the array amplitude distribution and the specified distribution;

5. The results of comparison are used to adjust the array parameters;

6. Steps 3, 4, 5 of this procedure may be repeated until the requirements are met.

IV. Experiment

In Ref. [3], an experiment of four models containing 10-element circumferential arrays is described. The four models are divided into two groups: one consists of equal-phase linear arrays and the other consists of unequal-phase arrays. The experimental results show that the phase-compensation method used to correct the ray path difference caused by the cylindrical surface is effective in reducing the side-lobes.

On the basis of the method proposed in this article, the authors have developed a computer-aided analysis and design program. This program has been used to design, fabricate, and test a 10x10 element surface-array model

which takes into account the coupling effects between elements and whose sidelobe level is lower than 22 dB. The array is fed by a comb-shaped network (Fig. 8); each feed of the axial array is equipped with an impedance-conversion unit for power distribution. The H-field and E-field directivity patterns of the array model are shown in Fig. 9 and Fig. 10, respectively. The H-field pattern shows that the proposed design procedure is effective for axial arrays. But the E-field pattern shows a shoulder on either side of the main lobe; this is caused by the T-junctions in the comb-shaped feed network which produce symmetric phase differences between the axial arrays.

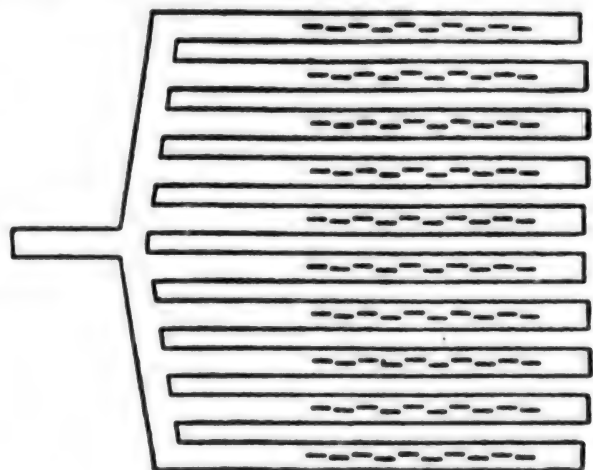To solve this problem requires further investigation of the effects of T-junctions.

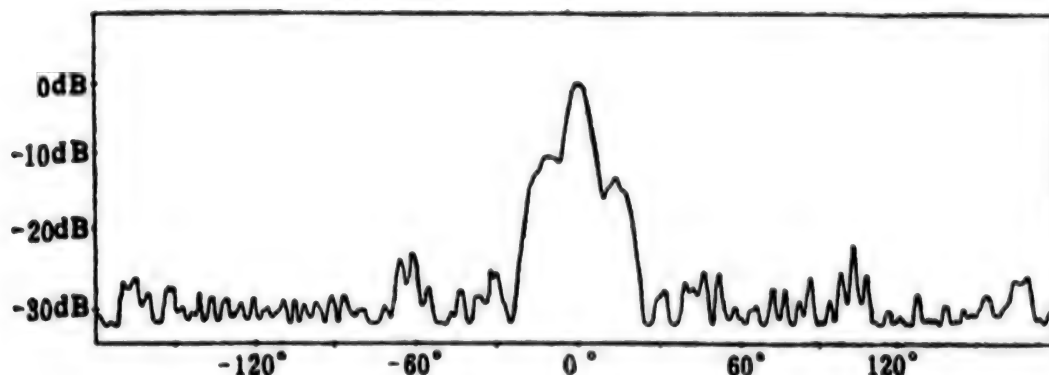Figure 8. Comb-Shaped Feed Network and Slot Positions

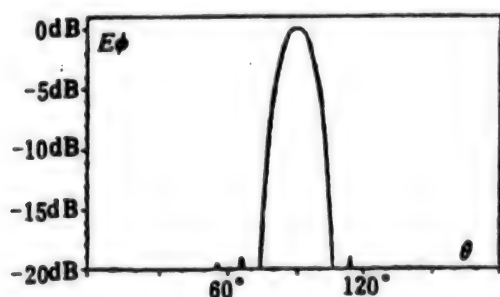Figure 10. E-Field Directivity Pattern of a 10x10 Surface Array

Figure 9. H-Field Directivity Pattern of a 10x10 Surface Array

References

[1] Zheng Jingliang et al, "Fields of Axial Magnetic Point Source on the Surface of Conducting Cylinder Covered by a Dielectric Layer", Proc. of 1985 Int. Symp. on Antennas and EM Theory, Beijing, pp 359-363.

[2] Zheng Jingliang et al, "Fields of Axial Slots on Conducting Cylinder Covered by Dielectric Layer", Proc. of 1987 Antenna Conference, Nanjing, Electronics Society, pp 11c(1) 1-4.

[3] Zheng Jingliang et al, "Experimental Study of Circumferential Conformal Slot-Array Antenna on Large Cylinder Covered by Dielectric Layer", QINGHUA DAXUE XUEBAO [JOURNAL of QINGHUA UNIVERSITY], Vol 27, No. 4, pp 82-87, Aug 1987.

[4] Zheng Jingliang et al, "Coupling Effects Between Axial Slots on Conducting Cylinder Covered by Dielectric Layer", DIANZI KEXUE XUEKAN [JOURNAL OF ELECTRONICS].

[5] Zheng Jingliang, "Internal Coupling between "Slots of a Rectangular Waveguide", Proc. of 1987 Graduate Student Communications Conference, Chengdu, Electronics Society and Communications Society, pp 514-519.

[6] Zheng Jingliang et al, "Slot Antenna on Large Conducting Cylinder Covered by a Dielectric Layer", Proc. of 1989 Int. Symp. on Antenna and EM Theory, Shanghai, pp 470-473.

UTD Formula for an Impedance Wedge

[Article by Wang Bingzong [3769 4426 0022] of the University of Electronic Science and Technology, Chengdu]

[Text] Abstract: A uniform GTD [geometrical theory of diffraction] formula for a TM plane wave diffracted by a conducting wedge whose illuminated side is an impedance surface is presented. This formula is used to compute the back-scatter radar cross-section (RCS) of a rectangular flat plate coated with lossy dielectric material. The calculated results are shown to be in good agreement with experimental measurements.

I. Introduction

To obtain a solution to the problem of high-frequency diffraction by a wedge with an impedance surface (e.g., aircraft wing and tail coated with absorption materials) has important practical applications. The uniform theory of diffraction (UTD)[1] has been widely and successfully applied to treat many high-frequency diffraction problems for a perfect conductor wedge[2]. Because the theory provides a clear physical concept and leads to a simple computational procedure, attempts have been made to extend the theory to solve diffraction problems for a wedge with impedance surface or a dielectric wedge[3-6], but the attempts have not been successful either because the derivations are not rigorous or because the resulting computational procedures are too complicated. In this article, motivated by the need for a concise UTD formula derived on the basis of rather rigorous analysis, we present a UTD formula for a wedge

surface illuminated by a TM plane wave (the illuminated surface is an impedance surface, not a perfect conductor).

II. UTD Formula for an Impedance Wedge

As shown in Fig. 1, consider an infinitely long wedge whose exterior angle is $n\pi$, and an incident TM plane wave with unit amplitude which makes an angle φ_0 with the wedge. The incident electric field is:

$$E^{in} = a_z \exp[jk\rho\cos(\varphi - \varphi_0)] \qquad (1)$$

where κ is the free-space propagation constant, a_z is a unit vector along the z axis, and (ρ, φ) are the polar coordinates of a field point. Assume that the plane wave only illuminates the surface A of the wedge $(\varphi = O)$, i.e., $\varphi_0 < n\pi - \pi$. Also assume that the surface impedance of A is Z_0/η_A and surface B $(\varphi = n\pi)$ is a perfect conductor. Z_0 is the free-space impedance.
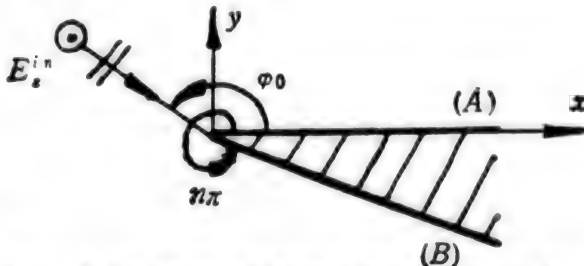

Figure 1. An Impedance Loading Wedge Illuminated by a TM Plane Wave

The reflection coefficient of the surfaced A is defined as

$$\Gamma_A = E_z^s / E_z^{in}\big|_{\varphi=0} \qquad (2)$$

where E_z^s is the scatter field. Thus, the reflection coefficient can be determined from the following formula:

$$\Gamma_A = \frac{Z_0/\eta_A - Z_0\sec(\varphi - \pi/2)}{Z_0/\eta_A + Z_0\sec(\varphi - \pi/2)} = \frac{\sin\varphi_0 - \eta_A}{\sin\varphi_0 + \eta_A} \qquad (3)$$

The boundary conditions can be written as:

$$\begin{cases} E_z^s = \Gamma_A E_z^{in}, & \varphi = 0 \qquad (4) \\ E_z^s + E_z^{in} = 0, & \varphi = n\pi \qquad (5) \end{cases}$$

By using the formula (see Appendix)

$$\exp(jk\rho\cos\Phi) = (2/\pi)\int_0^\infty K_{i\mu}(jk\rho)\mathrm{ch}[\mu(\pi - |\Phi|)]d\mu \qquad (6)$$

equation (1) can be expressed in the following integral form:

$$E_z^{in} = (2/\pi)\int_0^\infty K_{i\mu}(\gamma\rho)\mathrm{ch}[\mu(\pi - |\varphi - \varphi_0|)]d\mu \qquad (7)$$

where $\gamma = \iota\kappa$. Assume that the scatter field has a corresponding solution in integral form:

$$E_z^s = (2/\pi)\int_0^\infty K_{i\mu}(\gamma\rho)[f_1(\mu)\mathrm{ch}\mu\varphi + f_2(\mu)\mathrm{sh}\mu\varphi]d\mu \qquad (8)$$

where the functions $f_1(\mu)$, $f_2(\mu)$ are determined from boundary conditions.

Substituting equations (7), (8) into the boundary conditions (4), (5), one obtains:

$$\begin{cases} \int_0^\infty K_{i\mu}(\gamma\rho)f_1(\mu)d\mu = \Gamma_A\int_0^\infty K_{i\mu}(\gamma\rho)\mathrm{ch}[\mu(\pi - \varphi_0)]d\mu \qquad (9) \\ \int_0^\infty K_{i\mu}(\gamma\rho)\{f_1(\mu)\mathrm{ch}(\mu n\pi) + f_2(\mu)\mathrm{sh}(\mu n\pi) + \mathrm{ch}[\mu(\pi - n\pi + \varphi_0)]\}d\mu = 0 \qquad (10) \end{cases}$$

Since equations (9), (10) must hold for any value of ρ, it follows that:

$$\begin{cases} f_1(\mu) = \Gamma_A\mathrm{ch}[\mu(\pi - \varphi_0)] \qquad (11) \\ f_1(\mu)\mathrm{ch}(\mu n\pi) + f_2(\mu)\mathrm{sh}(\mu n\pi) + \mathrm{ch}[\mu(n\pi - \pi - \varphi_0)] = 0 \qquad (12) \end{cases}$$

Equations (11), (12) can be solved for $f_1(\mu)$, $f_2(\mu)$, which are substituted into equations (8) to give:

$$E_z^s = \Gamma_A E_{z,A}^s - E_{z,B}^s \qquad (13)$$

where

$$E_{z,A}^s = \frac{1}{\pi}\int_0^\infty K_{i\mu}(\gamma\rho)\left\{ \frac{\mathrm{sh}[\mu(n\pi + \pi - \varphi - \varphi_0)]}{\mathrm{sh}(\mu n\pi)} \right. $$
$$\left. + \frac{\mathrm{sh}[\mu(n\pi - \pi - \varphi + \varphi_0)]}{\mathrm{sh}(\mu n\pi)} \right\}d\mu \qquad (14)$$

$$E_{z,B}^s = \frac{1}{\pi}\int_0^\infty K_{i\mu}(\gamma\rho)\left\{ \frac{\mathrm{sh}[\mu(n\pi - \pi + \varphi - \varphi_0)]}{\mathrm{sh}(\mu n\pi)} \right. $$
$$\left. - \frac{\mathrm{sh}[\mu(n\pi - \pi - \varphi - \varphi_0)]}{\mathrm{sh}(\mu n\pi)} \right\}d\mu \qquad (15)$$

By subtracting the reflection field from the scatter field (13) and carrying out the necessary mathematical derivations, one can obtain the following integral expression for the diffraction field:

$$E_z^d = \Gamma_A E_{z,A}^d - E_{z,B}^d \qquad (16)$$

where

$$E_{z,A}^d = I(\pi + (\varphi - \varphi_0), k\rho) - I(\pi - (\varphi + \varphi_0), k\rho) \qquad (17)$$

$$E_{z,B}^d = I(\pi - (\varphi - \varphi_0), k\rho) - I(\pi + (\varphi + \varphi_0), k\rho) \qquad (18)$$

and the definition of the integral I is:

$$I(\delta, k\rho) = \frac{1}{2n\pi}\sin\left(\frac{\delta}{n}\right)\int_0^\infty \frac{\exp(-\gamma\rho\mathrm{ch}x)}{\mathrm{ch}(x/n) - \cos(\delta/n)}dx \qquad (19)$$

Under high-frequency conditions, $\kappa\rho \gg 1$; one can transform the integral (19) using the method of steepest descent to yield:

$$I(\delta, k\rho) \approx \frac{\exp(-jk\rho)}{2n\sqrt{2\pi jk\rho}}\mathrm{ctg}\left(\frac{\delta}{2n}\right)F\left[n^2\sin^2\left(\frac{\delta}{2n}\right)2k\rho\right] \qquad (20)$$

where the transition function F(x) is defined by [1]:

$$F(z) = 2j|\sqrt{z}| \ e^{iz} \int_{|\sqrt{z}|}^{\infty} e^{-it^2} dt \qquad (21)$$

Equation (20) can be used to derive an expression for the scatter field under high-frequency conditions, i.e., the UTD formula:

$$E_z^s = \frac{\exp(-jk\rho)}{2\pi\sqrt{2\pi jk\rho}} \left(\Gamma_s \left\{ \operatorname{ctg}\left[\frac{\pi+(\varphi-\varphi_0)}{2n}\right] F\left[n^2\sin^2\left(\frac{\pi+(\varphi-\varphi_0)}{2n}\right)2k\rho\right] \right. \right.$$
$$- \operatorname{ctg}\left[\frac{\pi-(\varphi+\varphi_0)}{2n}\right] F\left[n^2\sin^2\left(\frac{\pi-(\varphi+\varphi_0)}{2n}\right)2k\rho\right]\right\}$$
$$- \left\{ \operatorname{ctg}\left[\frac{\pi-(\varphi-\varphi_0)}{2n}\right] F\left[n^2\sin^2\left(\frac{\pi-(\varphi-\varphi_0)}{2n}\right)2k\rho\right] \right.$$
$$\left. \left. - \operatorname{ctg}\left[\frac{\pi+(\varphi+\varphi_0)}{2n}\right] F\left[n^2\sin^2\left(\frac{\pi+(\varphi+\varphi_0)}{2n}\right)2k\rho\right]\right\}\right) \qquad (22)$$

It can be shown that the results from equation (22) ensure that the overall field is continuous at the reflected and incident shadow boundaries.

When $\Gamma_A = -1$, equation (22) becomes the UTD formula for a perfect conductor wedge. In comparison with the conventional UTD formula for a conducting wedge given in Ref. [1], we find:

(1) The two formulas yield results with the same degree of accuracy;

(2) In practice, the UTD formula presented in this article is easier to use because for a given set of diffraction parameters n, φ, φ_0, this formula can be used to calculate the diffraction field of a conducting wedge directly, whereas the formula of Ref. [1] requires an extra step of calculating the intermediate parameter $N^{plus \ or \ minus}$ [1].

III. Numerical Example

The rectangular conducting plate is a basic structure commonly used in radar theory and antenna theory. In this example we shall use the UTD formula for an impedance wedge (equation (22)) to calculate the back-scattered radar cross section (RCS) for a rectangular conducting plate coated with lossy dielectric material, and compare the results with measured data.
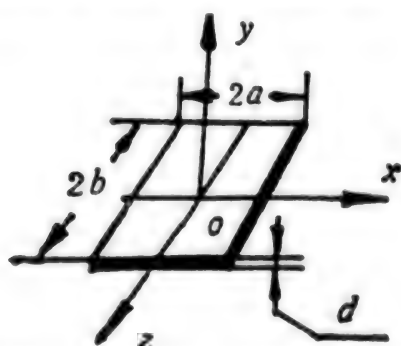

Figure 2. Rectangular Conducting Plate With One-Sided Coating

Consider a 2a x 2b rectangular plate located in the xoz plane. The plate is coated with a uniform layer of lossy dielectric material whose relative dielectric constant is $\varepsilon_r = \varepsilon'_r - j\varepsilon''_r$, and whose relative permeability is $\mu_r = \mu'_r - j\mu''_r$; let the thickness of the dielectric layer be denoted by d, as indicated in Fig. 2. Assume that the incident wave is a TM plane wave relative to the z axis, i.e., the electric field only has a z component. The angle of incidence relative to the y axis is θ_0, and the incidence plane is the xy plane.

The computational procedure is briefly summarized below:

(1) Under the approximation of geometric optics, the reflection coefficient of an infinite coated conducting plate Γ_A is [7]:

$$\Gamma_A = \frac{(\sqrt{\mu_r} \cos\theta_3 - \sqrt{\varepsilon_r} \cos\theta)\exp(j2k_y d) - (\sqrt{\mu_r} \cos\theta_3 + \sqrt{\varepsilon_r} \cos\theta)}{(\sqrt{\mu_r} \cos\theta_3 + \sqrt{\varepsilon_r} \cos\theta)\exp(j2k_y d) - (\sqrt{\mu_r} \cos\theta_3 - \sqrt{\varepsilon_r} \cos\theta)} \qquad (23)$$

where the complex angle θ and κ_y are determined from the following relations:

$$\begin{cases} \sin\theta_3 = \sqrt{\mu_r \varepsilon_r} \sin\theta & (24) \\ k_y d = 2\pi(d/\lambda)[\mu_r \varepsilon_r - \sin^2\theta_0]^{1/2} & (25) \end{cases}$$

λ is the free-space wavelength.

(2) By extending the rectangular plate indefinitely in the z direction, one can calculate the back-scattered RCS per unit length of this infinitely long coated strip.

$$\sigma_{length} = \lim_{\rho \to \infty} 2\pi\rho |E_z^s / E_z^{in}|^2 \qquad (26)$$

where the far-field scatter field E_z^s can be calculated from the UTD formula for an impedance wedge by treating the strip as an infinitely long wedge with an exterior angle of 2π.

(3) The back-scattered RCS of the rectangular plate can be calculated from the following formula [8]:

$$\sigma_{plate} = (8b^2/\lambda)\sigma_{length} \qquad (27)$$

Fig. 3 shows the calculated back-scattered RCS of a square aluminum plate coated with Eccosorb FDS radar-absorbing material; the figure also shows the measured data from Ref. [9]. The calculated values are seen to be in good agreement with measured data, and the agreement improves as the electrical dimension of the object increase (i.e., at higher frequency).

Although the maximum electrical dimension of the object in Fig. 3 is only 3λ (located at the low end of the resonance region), the agreement between calculated and measured values is already quite good. It can be expected that in the high-frequency region (electrical length greater than 10λ (located at the low end of the resonance
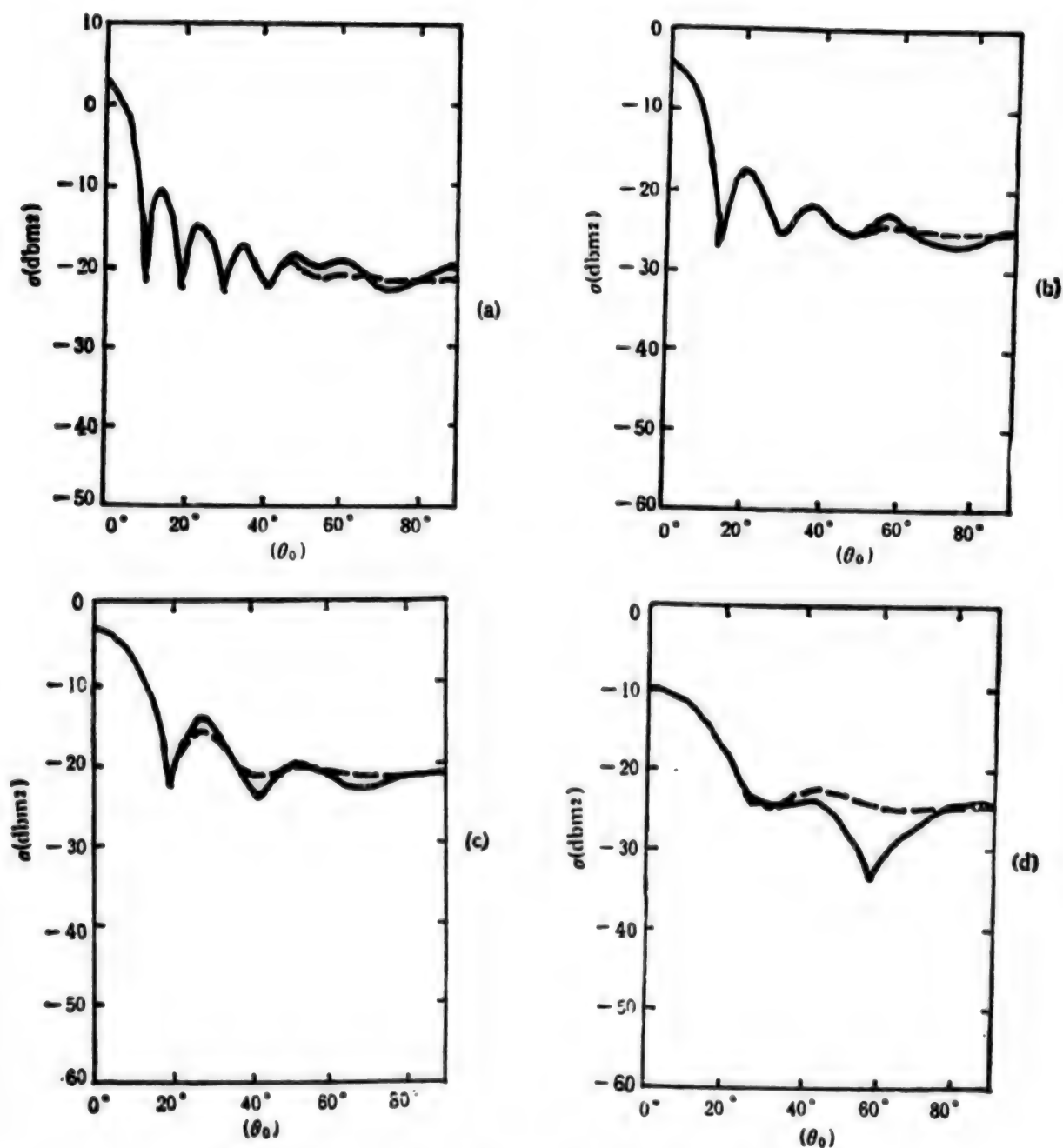
(a) $f = 6\text{GHz}$ $d = 0.762\text{mm}$ $2a \times 2b = 15\text{cm} \times 15\text{cm}$
(b) $f = 6\text{GHz}$ $d = 0.762\text{mm}$ $2a \times 2b = 10\text{cm} \times 10\text{cm}$
(c) $f = 3\text{GHz}$, a, b, d same as (a)
(d) $f = 3\text{GHz}$, a, b, d same as (b)

Figure 3. Back-Scattered Radar Cross Section for a Square Aluminum Plate With Single-Sided Coating.
- - - calculated results of this article. —— measured values from Ref. [9]

region), the agreement between calculated and measured values is already quite good. It can be expected that in the high-frequency region (electrical length greater than 10 λ), the RCS value computed from the UTD formula will be in better agreement with the true RCS value.

This example also shows that while the UTD formula for an impedance wedge is a formula based on high-frequency approximation, it sometimes can also be used in a broader region such as the resonance region.

Appendix

Proof of Formula (6)

Based on the formula [6.794(1)] of Ref. [10],

$$\int_0^\infty K_{i\nu}(a)K_{i\nu}(b)\mathrm{ch}[(\alpha-\varphi)x]dx = \frac{\pi}{2}K_0(\sqrt{a^2+b^2-2ab\cos\varphi}) \tag{A1}$$

one obtains

$$\pi^2/(4j)H_0^{(2)}(kR) = (\pi/2)K_0(jkR)$$
$$= (\pi/2)K_0[\sqrt{(\gamma\rho)^2+(\gamma\rho_0)^2-2\gamma^2\rho\rho_0\cos(\varphi-\varphi_0)}\;]$$
$$= \int_0^\infty K_{i\nu}(\gamma\rho)K_{i\nu}(\gamma\rho_0)\mathrm{ch}[\mu(\alpha-|\varphi-\varphi_0|)]d\mu \tag{A2}$$

By letting $\rho_0 \to \infty$, and utilizing the asymptotic expression of $H^{(2)}_0(z)$, $K_\nu(z)$:

$$H_0^{(2)}(z)\xrightarrow{|z|\to\infty}\sqrt{2j/(\pi z)}\exp(-jz) \tag{A3}$$

equation (A2) becomes

$$K_\nu(z)\xrightarrow{|z|\to\infty}\sqrt{\pi/(2z)}\exp(-z) \tag{A4}$$

$$\frac{\pi^2}{4j}\sqrt{\frac{2j}{\pi k\rho_0}}e^{-jk\rho_0(1-\rho\cos(\varphi-\varphi_0))}$$

$$\approx \int_0^\infty K_{i\mu}(\gamma\rho)\sqrt{\frac{\pi}{2j k\rho_0}}e^{-jk\rho_0}\mathrm{ch}[\mu(\alpha-|\varphi-\varphi_0|)]d\mu$$

Therefore,

$$\exp[jk\rho\cos(\varphi-\varphi_0)] = (2/\pi)\int_0^\infty K_{i\mu}(\gamma\rho)\mathrm{ch}[\mu(\alpha-|\varphi-\varphi_0|)]d\mu \tag{A5}$$

or

$$\exp[jk\rho\cos\phi] = (2/\pi)\int_0^\infty K_{i\mu}(\gamma\rho)\mathrm{ch}[\mu(\alpha-|\phi|)]d\mu \tag{6}$$

References

[1] R. G. Kouyoumjian, P. H. Pathak, Proc. IEEE, 62(1974), 1448-1461.

[2] R. C. Hansen, et al., Geometric Theory of Diffraction, IEEE Press, New York, 1981.

[3] W. D. Burnside, K. W. Burgener, IEEE Trans. on AP, AP-31(1983), 104-110.

[4] K. C. Chamberlin, R. J. Luebbers, IEEE Trans. on AP, AP-30(1982), 1093-1098.

[5] R. J. Luebbers, IEEE Trans. on AP, AP-32(1984), 70-76.

[6] R. Tiberio, G. Pelosi, G. Manare, IEEE Trans. on AP, AP-33(1985), 867-873.

[7] J. R. Wait, Electromagnetic Waves in Stratifield Media, Academic Press, New York, 1980.

[8] R. A. Ross, IEEE Trans. on AP, AP-14(1966), 329-335.

[9] Steven W. Rogers, AD-A170973(1986).

[10] I. S. Gradshteyn, I. M. Ryzhik, Table of Integrals, Series, and Products, Academic Press, New York, 1980.

Using Li-Like Al Ions in Laser Plasmas to Achieve Soft X-Ray Amplification

[Article by Lu Peixiang [7120 1014 6116], Zhang Zhengquan [1728 2973 3123], Fan Pinzhong [5400 0756 1813] and Xu Zhizhan [1776 5267 1455] of Shanghai Institute of Optics and Fine Mechanics [SIOFM], Chinese Academy of Sciences: "Using Li-Like Al Ions in Laser Plasmas to Achieve Soft X-Ray Amplification." Originally published in JPRS-CST-90-012, 18 Apr 1990 pp 20-21; rerunning to provide corrected term.]

[Text] Key words: Laser Plasma, Soft X-Ray Spontaneous Radiation Amplification

Soft X-ray amplification is an interesting research area. Jaegle, et al., have already done some work to achieve soft X-ray amplification using Li-like ions.[1] This paper is a report of the results recently obtained in our laboratory.

I. Experimental

This experiment was carried out with an intense six-beam neodymium laser. The output energy of each beam was approximately 10 J and the pulse width was about 250 ps. Two laser beams 200 ps apart travel along the same optical axis through a cylindrical lens (R = 200 mm) and a F/1.5 non-spherical lens (f = 90 mm) which focus them onto a flat aluminum target. The focal line was 8 mm long and 200 μm wide. The mean light intensity was 2×10^{12} W/cm^2. In a previous experiment[2], we noticed the presence of a large-scale plasma jet structure between the hot plasma and cold target. In order to avoid this boundary effect to ensure the homogeneity of the entire plasma line, the width of the target (i.e., the length of the plasma) was chosen to be smaller than the length of the focal line. In this experiment, it was 6.3 mm.

The emission spectrum was observed using a 1-m stigmatic grazing-incidence-grating spectrograph[3] (grating spacing: 1/2400 mm, wavelength accuracy: 0.05 Angstrom, one-dimensional resolution: 50 μm) developed by our group. The spectral range observed was 10-120 Angstroms. The spectrum was recorded using a soft X-ray film manufactured in Shanghai. The darkness scan curve of the spectrum was obtained using a Japanese-made MP-3 microphotometer.

The direction of the focal line was varied by rotating the cylindrical lens in order to observe the axial and non-axial (approximately 45° angle) emission spectra of the aluminum target.

Figure 1 shows the axial and non-axial darkness scan curves of the linear plasma. At 105.7 Angstroms the intensity changes significantly, which corresponds to a strong spontaneous radiation amplification effect.
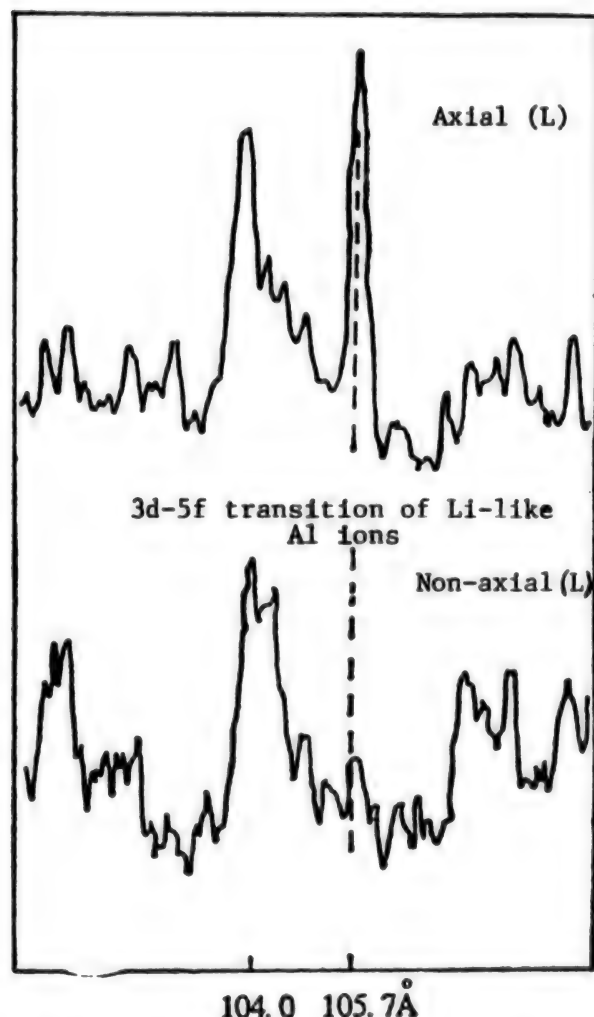
3d-5f transition of Li-like
Al ions

**Figure 1. Linear Plasma Spectra Observed Along Axial
and Non-Axial Direction; aluminum target: linear
plasma 6.3 mm long, 200 µm wide**

II. Results and Discussion

1. Figure 1 clearly shows that the 105.7 Angstrom line
was very intense when the linear plasma was observed
along its axis. However, this line disappeared and
became the background of the spectrum in non-axial
observation. Experimentally obtained emission spectra
of aluminum plasmas[4] show that there are no other
spectral lines near 105.7 Angstroms; there is only the
3d-5f transition of Li-like aluminum ions.[5] This indi-
cates that the 3d-5f Li-like aluminum transition in the
soft X-ray band, i.e., at 105.7 Angstroms, undergoes
spontaneous radiation amplification.

2. Using the following approximate formula for plasma
temperature[6]

$$\frac{T}{1\,\mathrm{keV}} = 0.6 \left[\frac{1}{t} \left(\frac{I_{abs}}{10^{14}\,\mathrm{W/cm^2}} \right) \cdot \left(\frac{\lambda_L}{1\,\mu m} \right)^3 \right]^{2/3}, \quad (1)$$

we roughly estimated that the plasma temperature was
approximately 60 eV. We assume that the temperature is
1 keV when the absorbed light intensity $I_{abs} = 10^{14}\,\mathrm{W/}$
$\mathrm{cm^2}$ and $I_{abs} = 0.7\ I$. This relatively low temperature is
just right for helium-like aluminum ions to become
Li-like aluminum ions through three-particle recombina-
tion in order to create population inversion.

From the spectrum taken along the axis, we found that
the one-dimensional spatial distribution of the 105.7
Angstrom spectral line is shorter than other spectral
lines. Moreover, its intensity peaks approximately 400
µm from the target surface. This may indicate that the
intensity peak is located in the medium-density zone
because plasma density decreases with increasing dis-
tance from the target.[7] This also indicates that the
optimal condition for the rapidly adiabatically cooled
plasma to produce a laser line at 105.7 Angstroms, i.e.,
the optimal recombination condition, is behind the
presence of the driving laser pulse.

3. The simple equation to calculate the gain factor is[8]:

$$I = Se^{GL} \qquad (2)$$

In approximation, we get I/S = 3.5 from the curve.
Hence, the gain factor was roughly estimated to be 2/cm.
Here, the source function was assumed to be the 105.7
Angstrom line intensity when observed non-axially. I is
the intensity of the line when observed axially.

This is an important study. In order to further verify this
effect, much work must be done. For instance, one needs
to obtain a gain curve by varying the length of the plasma
in order to demonstrate that the intensity of the 105.7
Angstrom (3d-5f) Li-like line increases non-linearly with
the length of the plasma.

References

1. Jaegle, P., Jamelot, G., et al., J OPT SOC AM B, 4, 563
(1987).

2. Xu Zhizhan, Jiang Zhiming, et al., OPT COMMU, 69,
49 (1988).

3. Zhang Zhengquan, Fan Pinzhong, et al.,
GUANGXUE XUEBAO [ACTA OPTICA SINICA], 8,
762, (1988).

4. Kelly, R.L., et al., NRL Report, 7599.

5. Guennou, H. and Sureau, A., Annual Report of Greco Interaction Laser-Matiere, 151, 1979.

6. Balian, R. and Adam, J.C., Session XXXIV, 1980 Interaction Laser-Plasmas (ed. Les Houchs), North-Holland Publishing Company, 307, 1982.

7. Jiang Zhiming [3068 1807 2494], Xu Zhizhan, et al., WULI XUEBAO [ACTA PHYSICA SINICA], (to be published).

8. Li Fuli [2621 4395 0448], "Laser Physics," China University of S&T Press, 1987.

Future of Lasers Is Crystal Clear

40100041b Beijing CHINA DAILY in English 2 Apr 90 p 2

[Text] Chinese scientists have developed a new crystal which has been used successfully in manufacturing small lasers, CHINESE SCIENCE NEWS reported in Beijing on Saturday [31 March 1990].

Developed by researchers from the Fujian Institute of the Structure of Matter, Chinese Academy of Sciences, the crystal, NYAB [neodymium yttrium aluminum borate], has been used by Japan's Hoya Corporation in its successful development of a green-light wavelength semiconductor laser.

"The power of the new NYAB laser is six times stronger than conventional infrared lasers and can be used in the production of disks, color printing machines and color photocopying machines," the report said. Because of its fine properties and much lower price, NYAB is highly competitive and is expected to take a firm hold in the international market. Hoya Corporation predicts that the application of NYAB in its color photocopying machines will results in sales of 500 million yuan a year. It has signed a contract with the Fujian Institute of the Structure of Matter to buy at least $50,000 worth of NYAB crystals a year. The institute has also sold NYAB in Europe and the United States.

Theory, Experimental Study of Nonlinear Active Multifunctional Crystal NYAB Laser

40090009a Shanghai GUANGXUE XUEBAO [ACTA OPTICA SINICA] in Chinese Vol 10 No 2, Feb 90 pp 103-108

[English abstract of article by Yang Aiping [2799 1947 5493], et al., of the Optics Department, Shandong University, Jinan; Shao Zongshu [6730 1350 2579], et al., of the Institute of Crystal Material, Shandong University, Jinan]

[Text] In this paper, a new theoretical mode of a multi-functional crystal laser is reported. The coupling wave-rate equations were established by using slowly varying amplitude approximation. The NYAB laser was modeled with a computer, and theoretical results were obtained. The threshold value and peak power of the lasers are discussed. The NYAB laser multifunctional effect was then studied by pumping a giant pulsed laser (λ = 589 nm) with an output peak power at 530 nm of 37.5 kW. Although the theoretical results coincided with the experimental ones, the deviation between the theoretical results and experimental ones was studied and proposals for improving multifunctional lasers were raised.

References

1. Liu Enquan, et al., ACTA OPTICA SINICA, Vol 7 No 2, Feb 1987 pp 139-143.

2. Karpenko, S.G., et al., SOV J QUANTUM ELECTRON, Vol 9 No 3, Mar 1979 pp 265-269.

3. Dmitriev, V.G., et al., SOV J QUANTUM ELECTRON, Vol 8 No 11, Nov 1978 pp 1356-1361.

4. Shen Yuanrang, "Principles of Nonlinear Optics," Science Press, Beijing, 1987, pp 46-56.

5. Zhou Bingkun, et al., "Principles of Lasers," National Defense Press, Beijing, 1984, pp 210-226.

6. Wang Jun, et al., M.A. Thesis, Shandong Univ., 1986.

7. Liu Mingguo, et al., M.A. Thesis, Shandong Univ., 1989.

8. Armstrong, J.A., et al., PHYS REV, Vol 127 No 6, Jun 1962 pp 1918-1939.

Phase Separation, Crystallization in Fluorozirconate Glasses

40090009b Shanghai GUANGXUE XUEBAO [ACTA OPTICA SINICA] in Chinese Vol 10 No 2, Feb 90 pp 109-113

[English abstract of article by Li Ruihua [2621 3843 5478] and Gan Fuxi [1626 4395 3588] of Shanghai Institute of Optics and Fine Mechanics, Chinese Academy of Sciences; Chen Jinqing [7115 6855 1987] of the Department of Material Science and Engineering, Zhejiang University, Hangzhou]

[Text] Optical waveguide fluoride glasses face a number of difficult problems despite their potential for ultra-low loss. One of the most serious is the scattering loss from defects, such as inclusions, phase separation particles and crystallites. By means of a Leitz optical microscope, X-ray diffraction, transmission electron microscope (TEM) and differential thermal analysis (DTA), the authors have investigated the phase separation and crystallization phemonema in ZrF_4-BaF_2-LaF_3-AlF_3 fluoride glasses. Phase separated particles, which formed via the nucleation and growth mechanism have been observed in the glass. The crystallites in the glass have been

confirmed to be β-BaF$_2$.ZrF$_4$ and α-BaF$_2$.2ZrF$_4$. The activation energies of crystallization of these phases have been determined by DTA.

References

1. Parker, J.M., et al., MATERIAL SCIENCE FORUM, Vol 5 (Complete Volume Proceedings of the Third International Symposium on Halide Glasses, held in Rennes, Franc, June), 1985 pp 257-262.

2. Bansal, N.P., et al., MATER RES BULL, Vol 19 No 5, May 1984 p 577.

3. Augis, J.A., Benett, J.E., THERMAL ANALY, Vol 13 No 8, Aug 1978 p 283.

4. Sun Hongwei, et al., JOURNAL OF THE CHINESE SILICATE SOCIETY, Vol 13 No 4, Dec 1985 p 408.

Study of Electron Density in High Power CW Transverse-Flow CO$_2$ Laser

[English abstract of article by Mao Yingli [3029 5391 4539], et al., of Shanghai Institute of Optics and Fine Mechanics, Chinese Academy of Sciences]

[Text] Measurements of the electron density in a 5 kW CW transverse-flow CO$_2$ laser gas discharge are presented. Experiments were performed with a single Langmuir probe. The electron density was evaluated using P.R. Smy's expression for a flowing plasma. The spatial distribution of the electron density and an analysis using the electron continuous equation are given. Under the conditions of pressure of 42 Torr and discharge current of 20 A, the electron density is approximately 3×10^{11} cm^{-3} and, along the flow, the distribution is nonhomogeneous, with the maximum value occurring 3 cm from the top edge of the anode in the flow direction. An explanation of the experimental results is given by the continuity formulation of electrons, and the theory coincides with the experiment.
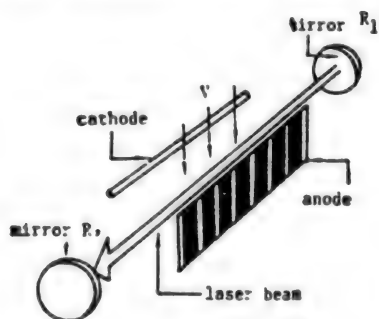

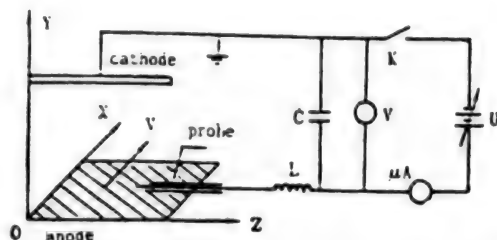**Figure 1. The Discharge Region of 5 kW CW Transverse-Flow CO$_2$ Laser**

Figure 2. The Electron Density Measurement Set-up
U: variable power supply, 0-1200 V; C: isolation capacitor; L: filter inductor

References

1. Smy, P.R., ADVANCES IN PHYSICS, Vol 25 No 5, May 1976 pp 517-553.

2. Seguin, V.A., et al., J APPL PHYS, Vol 60 No 9, Nov 1986 pp 3088-3092.

3. Lowke, J.J., et al., J APPL PHYS, Vol 44 No 10, Oct 1973 pp 4664-4671.

4. Witteman, W.J., "The CO$_2$ Laser," Springer-Verlag, 1987, pp 150-151.

5. Akiba, T., et al., LASER RESEARCH, Vol 4 No 3, Dec 1976 pp 242-248.

6. Cheng Zhaogu, et al., CHINESE JOURNAL OF LASERS, Vol 10 No 12, Dec 1983 pp 821-825.

7. Von Engel, A., "Ionized Gases," Oxford, Clarendon Press, 1965, p 218.

8. Cherrington, B.E., "Gaseous Electronics and Gas Lasers," Pergamon Press, 1979 pp 99, 115.

9. He Guangsheng, et al., "Laser Device Design Fundamentals," Shanghai Science and Technology Press, 1979, p 151.

Investigation of Rotating Speckle-Shearing Interferometry

[English abstract of article by Chen Bingquan [7115 3521 3123] and Jiang Jinhu [1203 6930 5706] of the Department of Physics, Suzhou University]

[Text] In this paper, a new method of dynamic speckle photography—rotating speckle-shearing interferometry—is proposed. The theoretical analysis and preliminary experimental results are presented. The advantage of this method is that the entire dynamic process of an object can be recorded on a single specklegram. In whole-field filtering, the deformation information at any instant can be obtained easily, and the images obtained are quite clear.

References

1. Chen Bingquan, et al., ACTA OPTICA SINICA, Vol 8 No 11, Nov 1988 pp 1018-1023.

2. Gu Jie, et al., ACTA OPTICA SINICA, Vol 7 No 5, May 1987 pp 394-399.

3. Zhu Yiqing, et al., ACTA OPTICA SINICA, Vol 5 No 11, Nov 1985 pp 1018-1025.

4. Goodman, J.W., "Laser Speckle and Related Phenomena," J.C. Dainty, ed., Science Press, Beijing, 1981, Chapter 2.

5. Hung, Y.Y., Durelli, A.J., J OF STRAIN ANALYSIS, Vol 14 No 3, 1979 pp 81-88.

6. Hung, Y.Y., Liang, C.Y., APPL OPT, Vol 18 No 7, Apr 1979 pp 1046-1050.

Double-Pulse TEA CO_2 Laser with Adjustable Pulse Interval

[English abstract of article by Li Xiangyin [2621 4161 6892], Sun Ning [1327 1337], et al., of the Department of Applied Physics, East China Institute of Technology, Nanjing]

[Text] A novel transversely excited atmosphere carbon dioxide laser is described in this paper. It is constructed by means of a common optical cavity. The device produces two pulses with an adjustable time interval of up to 150 µs under a single excitation, which is obtained without gas flow. The design features of the construction and the control circuit are presented, and the experimental results and conclusion are given.

References

1. Dzakowic, et al., J APPL PHYS, Vol 44 No 11, Jul 1973 pp 5061-5063.

2. Fox, J.A., APPL PHYS LETT, Vol 37 No 7, Oct 1980 pp 590-591.

3. Baranov, V.Yu., APPL OPTICS, Vol 19 No 6, Mar 1980 pp 930-936.

4. He Guangsheng, et al., "Laser Device Design Fundamentals," Shanghai Science and Technology Press, 1979, pp 186-188.

5. Zhang Diankun, et al., JOURNAL OF EAST CHINA INSTITUTE OF TECHNOLOGY, No 1, Mar 1984 pp 112-115.

6. Fu Lisi, "General Physics," Peoples Science Press, Beijing, 1964, pp 476-478.

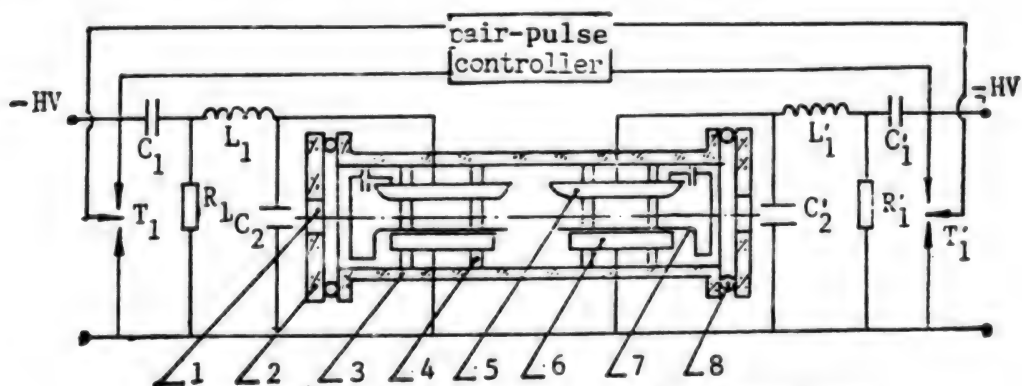7. Roper, V.G., et al., OPTICS COMMUN, Vol 25 No 2, May 1978 pp 235-240.

Figure 1. Schematic of Device Construction and Power Supply System

Key: 1. Mirror 2. End cover 3. Shell 4. Stand 5. Anode 6. Cathode 7. Preionization electrode 8. Seal ring

Millimeter-Wave Frequency Tripler Covering 210-270 GHz

[Article by Yang Yufen [2799 3768 5358]; of the Institute of Semiconductors, CAS, Beijing]

[Text] Abstract: A frequency tripler covering the 210-270 GHz band with a peak efficiency of 5.8 percent is described. The maximum output power occurs at an input power of 30-50 mW. The frequency tripler consists of a fundamental-wave input waveguide WR-12, an output waveguide WR-4, and a co-axial low-pass filter between the two waveguides.

1. Introduction

The invention of Gunn and IMPATT [Impact avalanche and transit time] devices has promoted the rapid growth of solid-state power sources. Today, Gunn devices have been designed to cover the 3-mm band (80-100 GHz), and IMPATT devices have been designed to cover the 2-mm band (130-150 GHz). However, in the higher frequency band of 200-500 GHz, no solid-state power source has become available. Although in theory sub-millimeter-wave oscillation can be achieved using quantum-well negative-resistance oscillators, the output power is too small to be of practical use. In the low-millimeter-wave and sub-millimeter-wave bands, the only way to develop a practical solid-state power source is to use a frequency multiplier. In order to solve the problem of designing local oscillators for low-millimeter-wave and sub-millimeter-wave receivers, significant progress has been made in recent years in the development of high-order frequency multipliers[1-3]. In this article, we shall introduce a frequency tripler covering the 210-270 GHz band with a peak efficiency of 5.8 percent.

2. Circuit Design

Increasing the efficiency of a millimeter-wave frequency tripler requires not only a varactor diode with ideal electrical parameters, but also a microwave circuit whose impedance must be conjugate-matched with the varactor at both input and output frequencies. In addition, there should be no power loss on the spatial frequency of the second harmonic, and a short circuit should exist at the second harmonic of the diode. Of course, to achieve impedance matching at both input and output frequencies is very difficult because the impedance of a varactor diode consists of two parts: a large capacitance and a relatively small resistance. In the frequency tripler we have developed, the zero-bias-voltage capacitance of the varactor diode is 13 fF, the series resistance is 9.3Ω, and the reverse breakdown voltage is 12.7V.

In the frequency tripler, a coaxial low-pass filter is located between two orthogonal input and output waveguides, and a varactor diode is placed at the peak-voltage point on the inside conductor of the low-pass

filter. Within the 210-270 GHz band, the geometric dimensions of all the elements of the coaxial filter are too small to install insulating sleeves; therefore, the inside and outside conductors must be precision-machined to ensure a high degree of concentricity in order to avoid short circuits. A bias filter with a simple, radially linear structure is placed at the upper coaxial section of the input waveguide. The geometric dimensions of the inside conductor of the bias filter have been increased to ensure concentricity and rigidity between the inside and outside conductors.

The low-pass filter between the input and output waveguides is designed to transmit all the input pump power to the varactor diode and to prevent the power of the frequency doubler and tripler from leaking into the input waveguide. In other words, looking from the varactor diode toward the filter, a short circuit exists at the input waveguide wall with respect to the frequency doubler and tripler. The impedances at the various nodes of the filter are:

$$Z_{max} = 70\Omega, \; Z_{min} = 9.9\Omega;$$

the five-node design provides good transmission characteristics.

In order to effectively transmit the pump power of the fundamental wave to the varactor diode, the impedance of the input waveguide must be matched with the input impedance of the filter. For this reason, the height of the input waveguide is reduced to 1/3 of the original height. In order for the second harmonics to be in a completely idle state, the cut-off frequency f_c of the input waveguide must be higher than the second-harmonic frequency of the input signal. In our design, we use the WR-4 waveguide as the output waveguide, which has a cut-off frequency of 173 GHz. To achieve better impedance-matching, the height of the output waveguide is reduced to 1/2 of the original height. Ideally, the waveguide height should be reduced further, but further reduction would make fabrication of the WR-4 waveguide (0.47x0.25 mm) too difficult. The varactor diode which is attached to the end of the low-pass filter should be completely enclosed inside the output waveguide. Figure 1 shows a schematic diagram of the entire frequency tripler, and Figure 2 shows the structure and dimensions of the low-pass filter.

In order to match the circuit impedance with the impedance of the varactor diode, it is necessary to carefully select the parameters of the contact filament, and to connect a short-circuit coaxial section in series with the varactor diode. Its length is 1/2 the wavelength of the output and 1/6 the wavelength of the input; its impedance is inductive in nature. This type of structure greatly improves the impedance matching for the varactor diode.

During the experiment, the output power can be maximized by adjusting the short-circuit device of the input and output waveguides. When changing the input base frequency, the same adjusting process can be repeated to optimize the output power at each frequency.
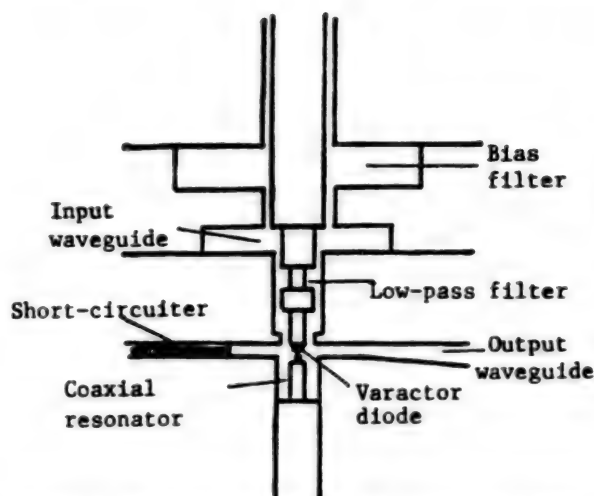
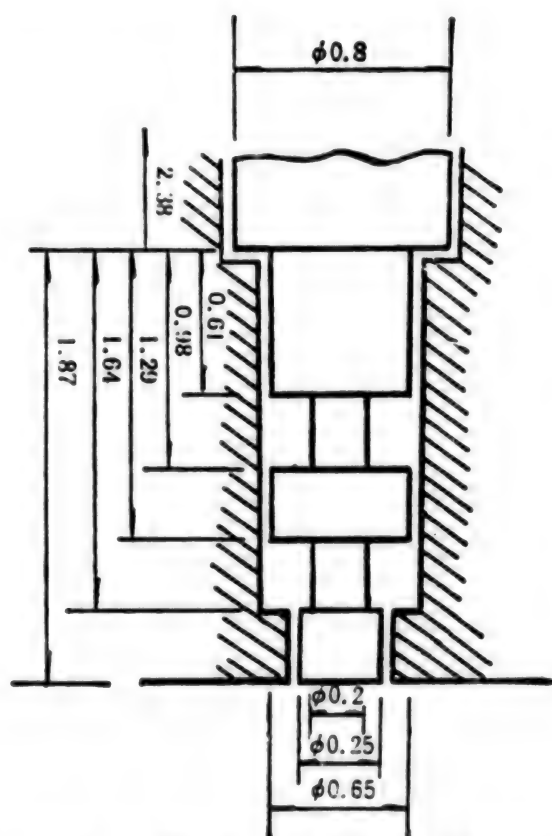Figure 1. Schematic Diagram of the Frequency Tripler

Figure 2. Structure and Dimensions of the
Low-Pass Filter

3. Experimental Results

In conjunction with adjusting the frequency of the input signal, the bias voltage of the varactor diode is also adjusted to maximize the output power. Specifically, the optimum state is achieved when the bias voltage of the varactor diode is 3-5V. The bias voltage is less than ½ the breakdown voltage. Figure 3 shows how the frequency multiplication efficiency varies with the output frequency. The efficiency reaches a peak value of 5.8 percent at a frequency of 250 GHz; beyond 250 GHz, the frequency multiplication efficiency drops sharply.
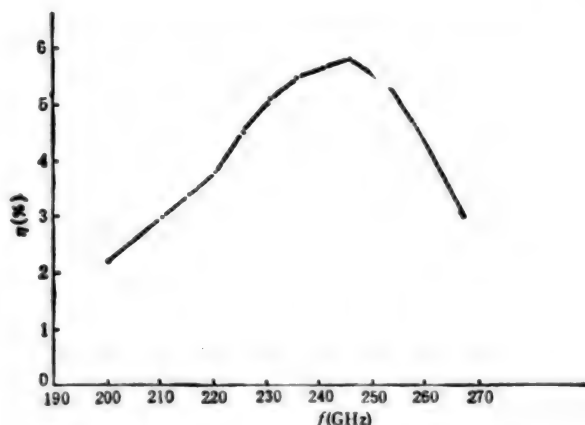

Figure 3. Variation of Frequency Multiplication
Efficiency With Output Frequency

4. Conclusion

The millimeter-wave frequency tripler which we have developed uses a coaxial filter to replace the microstrip-line filter designed by J. W. Archer[4]. The new design has many advantages including a simplified structure, easy fabrication, and improved reliability; it also yields very high efficiency in frequency multiplication. With this structure, a 2-mm signal with input frequency of 150 GHz can produce an output frequency of approximately 450 GHz. Therefore, the frequency tripler can provide a viable source of local oscillation for sub-millimeter-wave receivers.

References

1. J. W. Archer., IEEE Trans. on MTT, MTT-30 (1982), 1247.

2. N. R. Erickson, IEEE Trans. on MTT, MTT-29 (1981), 557.

3. J. W. Archer, Rev. Sci. Instr. 54 (1983), 1371.

4. J. W. Archer, IEEE Trans. on MTT, MTT-32 (1984), 416.

Depletion-Mode Selectively Doped GaAs Heterojunction Transistor Fabricated

[Article by Chen Dingqin [7115 1353 2953], Zhang Xiaoling [1728 2556 3781], Xiong Siqiang [3574 1835 1730], Gao Cuihua [7559 5050 5478] and Zhou Fan [0719 1581] of the Institute of Semiconductors, CAS, Beijing]

[Text] Abstract: A depletion-mode selectivity doped heterojunction transistor is designed and fabricated. The epitaxial modulation-doping material is grown in the Institute's FS-III-type MBE furnace. The electron mobility of the material by Hall measurement is typically 6500 $cm^2/v.s.$ at room temperature and 75,000 $cm^2/v.s$ at 77°K. The two-dimensional sheet electron density is 9×10^{11} cm^{-2}. The gate length of the low-noise depletion device is 1.2-1.5 µm and the width is 2x180 mS [milliSiemens per mm] at room temperature and can reach 200 mS/mm at 77°K.

1. Introduction

Selectively doped transistors have superior performance in terms of low noise, high frequency and high speed[1]. Such devices are made from molecular beam epitaxial (MBE) modulation-doping materials. In the selectively doped step-heterojunction structure which is composed of the undoped narrow-forbidden-band material GaAs and the doped n-type wide-forbidden-band material AlGaAs, the electrons move from AlGaAs to GaAs. Due to the potential barrier of the heterojunction, a two-dimensional electron gas (2DEG) is formed inside a 50-80-Angstrom thin layer near the interface. Within this layer, electrons can only move parallel to the interface; in the direction perpendicular to the interface, the energy-quantized electrons are constrained. In other words, the two-dimensional electron gas at the interface of GaAs and AlGaAs is spatially isolated form its ionized source; therefore, dispersion of ionized impurities is greatly reduced and electron mobility μ_n is increased. Devices with these characteristics will have a wide range of applications in high-speed data processing, microwave digital communications and satellites for television broadcasting.

2. Fabrication of the Device

In the fabrication of MBE materials, first a 1-µm undoped GaAs layer is grown on a substrate of Cr-doped GaAs (100) semi-insulating material; it is called the buffer layer. Then a 50-80-Angstrom-thick undoped AlGaAs layer is grown; this is called the isolation layer. Its function is to isolate the 2DEG spatially from its ionized source, so that the interacting Coulombic force between the ionized impurities in the doping source region and the electrons in the GaAs layer is minimized.

On top of this layer, silicon-doped, 500-700-Angstrom-thick, n-type AlGaAs active layer with an electron density of 1×10^{18} cm^{-3} is grown. Finally, an undoped, 200-Angstrom-thick GaAs protective layer is grown to facilitate Ohmic contact. Figure 1 shows the structure of the fabricated MBE material. The energy-band structure of this material is shown in Figure 2.
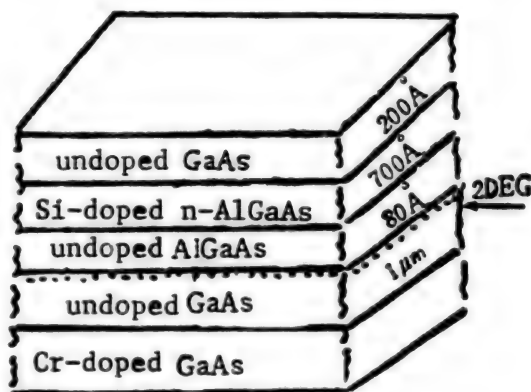

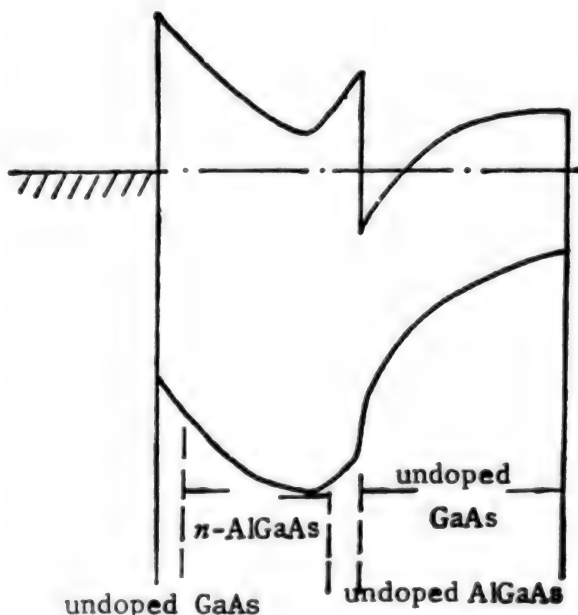**Figure 1. Structure of the MBE Material**

Figure 2. Energy-Band Diagram of the MBE Material

The MBE material produced in the FS-III furnace of this Institute is used in fabricating the device. Specifically, low-noise depletion-type GaAs heterojunction transistors with operating frequencies of 3.83 GHz and 1.5 GHz have been designed. The gate length of the isolation

device is $L_g = 1.2$-1.5 μm; the source-gate and drain-gate distances are: $L_{gs} = L_{dg} = 1.5$ μm, and the gate width is $W_g = 2 \times 180$ μm. By Hall measurement, the electron mobility of the MBE material is 6500 $cm^2/v.s$ at room temperature and 75,000 $cm^2/v.s.$ at 77°K. The two-dimensional sheet electron density $n_s = 9 \times 10^{11}$ cm^{-2} in the latter case.

The fabrication process consists of cleaning the MBE material with an organic solvent, and etching a 0.3-μm-high flat surface using a mixed solution of $NH_4OH + H_2O_2 + H_2O$ in order to isolate this area from the device's ionized active region.

A conventional photo-etching technique is used to determine the source and drain ohmic contact regions, and the source and drain contacts are peeled off by evaporating AuGeNi/Au contact metal. This metal is placed in a mixture of hydrogen and nitrogen at a temperature of 430°-470°C to form an alloy with the surface layer GaAs, which provides good source and drain Ohmic contacts.

In the gate region, a 300-Angstrom-deep groove is cut using the reactive ion etching (RIE) technique to reduce the parasitic resistance, and to form a 0.5-μm-thick AlTiAu gate electrode. Figure 3 shows the structure of the fabricated selectively doped heterojunction transistor.

3. Performance of the Device

Under room temperature, the d.c. transconductance of the depletion-mode heterojunction transistor is 110-130 ms/mm. From the transconductance formula $g_m = g_o (1 + R_s g_o)$, it can be estimated that the intrinsic transconductance g_o is approximately 170 ms/mm; R_s, the parasitic resistance between the source and gate, has a value of 2.8-3.3Ω. Figure 4 [photograph not reproduced] shows the d.c. characteristics of the device.

At 77°K, the transconductance of the transistor is 200 ms/mm, and its d.c. characteristics are shown in Figure 5. [photograph not reproduced].
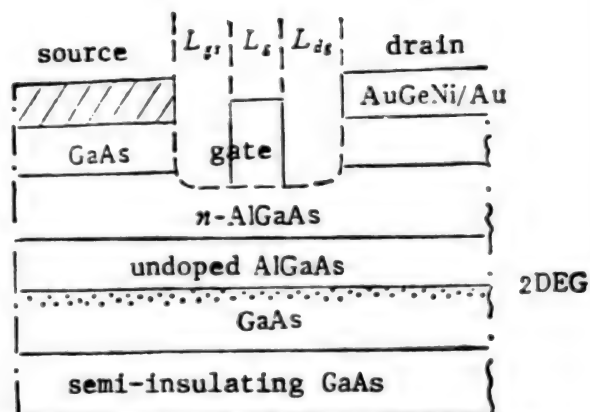
Figure 3. Schematic Diagram of the Depletion-Mode Selectively Doped Heterojunction Transistor

The operating frequency of this device meets the design requirements of 3.83 GHz and 1.5 GHz. The calculated noise figure is approximately 2-3 dB.

4. Concluding Remarks

At present, certain measures are being taken to improve the performance of the device. In particular, the following problems must be corrected: 1) The breakdown voltage V_G is too low, which may cause severe damage to the device; this problem is probably associated with the poor integrity of the MBE material. 2) The parasitic resistance R_s between the source and gate is too high; this problem may be corrected by using improved fabrication techniques. This device can be used on the receivers of communications satellites.

References

1. Paul M. Solomon, Hadis Morkoc, IEEE TRANS. ON ED, ED-31 (1984)8, 1015.

Recent Developments in Fiber-Optic Communications Described

Technical Indicators for Various Systems

[Article by Li Guangping [2621 1639 1627] and Zhong Genheng [4429 2704 1854]]

[Excerpt] [Passage omitted] The following is a brief introduction to the progress made in China's optical communications.

1. Significant Technical Progress Achieved

After over 10 years of effort, technology for optical communications systems below 34 Mb/s [DS3] (480 voice circuits) has matured. Moreover, it has been widely put into use. Experimental commercial 140 Mb/s [DS4] long-distance trunk lines and urban telephone relay systems have been installed in Wuhan and in Tianjin Municipality and between Hefei and Wuhu in Anhui Province. In the laboratory, we have successfully demonstrated a 112-km unrepeatered 34 Mb/s line and an 80.5-km unrepeatered 140 Mb/s line, both at a 1.55 μm wavelength. As for the 400 Mb/s [DS5, Japanese standard] (5760 voice circuits) single-mode fiber-optic transmission system, we have successfully demonstrated 30.7 km of unrepeatered transmission at 1.3 μm. In the laboratory, the transmission range of the 560 Mb/s [DS5, European standard] (7680 voice circuits) system has reached 50.5 km. The development of a faster-rate optical fiber (1.12 Gb/s) is under way. Studies on WDM (wavelength-division multiplexing) technology and coherent fiber-optic communications systems are also in progress. An experimental 100-km unrepeatered 560 Mb/s coherent fiber-optic communications system has been built.

In terms of optical-fiber fabrication technology, the use of an MCVD [modified chemical vapor deposition] technique to make multimode fiber has matured and has been transformed into industrial production. All specifications meet CCITT requirements. The mean attenuation is 0.7 dB/km (at 1.3 μm) and the bandwidth is 800-1000 MHz-km. Single-mode fiber fabrication technique is essentially under control. Its attenuation coefficients are 0.47-0.5 dB/km and 0.24-0.3 dB/km at wavelengths of 1.3 μm and 1.55 μm, respectively. We are developing a dispersion-shifted optical fiber to simultaneously minimize attenuation and dispersion, and other fibers for special applications.

In the development of optoelectronic devices and passive devices, over 50 varieties with various structures and applications have been developed; some of them have been put into small-batch production. A dual-active-layer, dual-channel, planar buried heterojunction (DAL-DC-PBH) dynamic single-longitudinal-mode 1.55-μm-wavelength laser diode (LD) has been successfully developed and used as the light source in an experimental 560 Mb/s fiber-optic communications system with an unrepeatered transmission range of 50 km. A DC-PBH laser diode with a minimum threshold current of 9 mA has a single-mode-operation linear power output that can reach 10-15 mW and a lifetime that has been improved from 50,000 to 100,000 hours. Research and development prototypes of surface-emitting and edge-emitting LEDs; long- and short-wavelength PIN-FET photo-receivers; and low-noise Si-APDs [avalanche photodiodes], Ge-APDs and InGaAs/InP-APDs have been evaluated.

Research on passive optical devices had a late start in China. We have nevertheless developed a variety of passive devices such as single-mode and multimode fiber connectors, optical drop-and-insert devices, optical switches, WDM devices, and fixed and variable attenuators. Their technical specifications are close to or have already met advanced international levels.

Some progress has been made in raw materials. In addition to satisfying domestic demand, $GeCl_4$, a dopant for InP single-crystal optical fiber, is being offered to foreign countries.

Technology in areas such as long-wavelength multimode optical fiber, single-mode optical fiber, optoelectronic devices, optoelectronic terminals and test instrumentation has reached an early 1980's level.

2. Applications

In China, research on fiber-optic communications began in 1974. Experimental fiber-optic lines were installed in the late 1970's; these experimental fiber-optic communications lines were installed in Beijing, Shanghai, Wuhan, Nanjing, Tianjin and Guilin. In 1981, there were over 120 fiber-optic communications systems registered with the CCITT in 118 countries and regions and China had three of them. Since the late 1980's, the pace of fiber-optic communications has picked up considerably. Fiber-optic communications systems, either developed independently or imported, have been placed in Shijiazhuang, Taiyuan, Datong, Changchun, Shenyang, Harbin, Guangzhou and other cities. In the Sixth 5-Year Plan, 331.5 km of optical cable, equivalent to 2,696 km of optical fiber, were laid for public networks.

In addition to the public networks, fiber-optic communications is also widely used in railroad communications, electric power switching, the petroleum industry, the military, industrial television, traffic management and computer networking. Based on available statistics, China has installed or plans to install 11,472.3 km

of optical cable. There are 110 systems with a bit rate higher than 8 Mb/s; approximately 70 percent of them are single-mode systems which are located in 8 provinces and 36 cities. The longest line is from Nanjing to Wuhan, 1,100 km in total length (140 Mb/s, imported, to be completed in 1990). The longest domestically manufactured system is from Hanyang to Jingzhou, 252 km in total length (34 Mb/s, already in operation).

Table 1 shows a list of fiber-optic communications systems at various bit rates. Table 2 shows technical specifications of domestically made fiber-optic communications systems.

Table 1

Bit rate	Number of systems
140 Mb/s	43
34 Mb/s	47
8 Mb/s	20

Table 2

Bit rate (Mb/s)	Device	Fiber	Wavelength (μm)	Relay range (km)
8	LED	Multimode	0.85	12
	LD	Multimode	1.3	39
34	LED	Single-mode	1.3	12
	LD	Single-mode	1.3	36
140	LD	Single-mode	1.3	30

In order to stimulate the growth of fiber-optic communications in China, the government arranged 15 demonstration projects in the Seventh 5-Year Plan. Most of these projects have been completed and the outcome is very encouraging. More progress in fiber-optic communications is expected in the Eighth 5-Year Plan.

National Statistics Provided

90FE0046B Beijing DIANXIN JISHU [TELECOMMUNICATIONS TECHNOLOGY] in Chinese No 2, Feb 90 p 47

[Article by Li Jiaju [2621 1367 7467]]

[Text] By the end of June 1989, there were 151 fiber-optic communications lines, 11,942 kilometers in total length, that were either already in operation, or under construction, or planned; 52 of these lines were imported and their total length is 6,755 kilometers.

1. Based on applications, they can be divided into 1) public-access lines: 78 municipal telephone lines, total length 3,007.60 km, and 27 long-distance lines, total length 5,965.52 km; and 2) dedicated lines: 8 lines, totaling 2,195.35 km, for railroad use; 20 lines for electric-power use, total length 221.70 km; 18 lines for other uses, total length 551.80 km.

2. Based on the transmission rate, they can be categorized as follows: 49 140-Mb/s lines, total length 8,059.54 km; 61 34-Mb/s lines, total length 2,982.07 km; 23 8-Mb/s lines, total length 464.56 km; and 18 other lines, total length 435.86 km.

Sino-Japanese Joint Venture

90FE0046C Beijing DIANXIN JISHU [TELECOMMUNICATIONS TECHNOLOGY] in Chinese No 2, Feb 90 p 47

[Article by Li Shen [2621 3947]]

[Text] Based on information released from the "Foreign Joint Venture Exhibit" recently held in Beijing, Xigu [6007 0657] Optical Fiber and Cable Corporation, a Sino-Japanese (Furukawa [Electric], Japan) joint venture, is formally in production. Changfei [7022 7378] Optical Fiber and Cable Ltd., a Sino-Dutch (Philips) joint venture, will be in production soon. After these two companies are in production, they will supply high-tech optical fibers and cables to improve telecommunications in China.

Influence on Light Absorption Spectra When Adding KCl to Silver Colloid

40090010a Beijing WULI XUEBAO [ACTA PHYSICA SINICA] in Chinese Vol 39 No 2, Feb 90 pp 177-182

[English abstract of article by Wang Weining [3769 5898 1337], Fang Yan [2455 3508] et al., of the Institute of Physics, Chinese Academy of Sciences, Beijing]

[Text] The influence on the light absorption when adding KCl to silver colloid is studied and compared with that when adding pyridine to the colloid. It is found that the light absorption increased due to the formation of an atomic cluster layer on the Ag particle surfaces caused by adding KCl, and that the plasmon resonance absorption of the original surfaces was reduced. At the same time, the linear-chain aggregation caused by adding KCl led to an apparent red shift of the plasmon resonance absorption, which sometimes was difficult to observe. The influence of these changes on SERS is also discussed.

References

1. Creighton, J.A., et al., J CHEM SOC FARADAY TRANS, Vol 275, 1979 p 790.

2. Pettinger, B., Krischer, K., J ELECTRON SPECTROS & RELAT PHENOM, Vol 45, 1987 p 133.

3. Hildebrandt, P., Stockburger, M., J PHYS CHEM, Vol 88, 1984 p 5935.

4. Lee, P.C., Meisel, D., J PHYS CHEM, Vol 86, 1982 p 3391.

5. Creighton, J.A., et al., in "Proceedings of International Raman Conf," W.F. Marphy, ed., North Holland, Amsterdam, 1980, p 398.

6. Merker, M., J COLLOID & INTERFACE SCI, Vol 105, 1985 p 5.

7. Fang Yan, et al., ACTA PHYSICA SINICA, Vol 39, 1990 p 46.

Effects of Light Feedback on CO_2 Laser Instabilities

40090010b Beijing WULI XUEBAO [ACTA PHYSICA SINICA] in Chinese Vol 39 No 2, Feb 90 pp 183-189

[English abstract of article by Zhang Ligen [1728 4539 2704], Chen Nanpeng [7115 2809 7720] et al., of the Institute of Modern Optics, Nankai University, Tianjin]

[Text] The effects of the transverse distribution of the light field on CO_2 laser instabilities are studied by means of light feedback. The phenomena of a pulsing frequency shift and chaos in the CO_2 laser caused by light feedback are observed experimentally. The mechanism of laser instabilities resulting from the transverse distribution is discussed.

References

1. Weiss, C.O., et al., OPT COMM, Vol 44, 1982 p 59; Weiss, C.O., J OPT SOC AM, Vol B2, 1983 p 137.

2. Arecchii, F.T., et al., PHYS REV, Vol A34, 1986 p 1617.

3. Lett, P., et al., J OPT SOC AM, Vol B2, 1985 p 1615.

4. Hoffer, L.M., et al., J OPT SOC AM, Vol B2, 1985 p 102.

5. Holzner, R., et al., PHYS REV, Vol A36, 1987 p 1280.

6. Casperson, L.W., IEEE J QUANTUM ELECTRON, Vol QE-14, 1978 p 756.

7. Brun, E., et al., J OPT SOC AM, Vol B2, 1985 p 156.

8. Biswas, D.J., et al., PHYS REV, Vol A35, 1987 p 456.

9. Dangoisse, D., et al., PHYS REV LETT, Vol 57, 1986 p 2657.

10. Chen, Lixue, et al., J OPT SOC AM, Vol B5, 1988 p 1160.

11. Lippi, G.L., Abraham, N.B., PHYS REV, Vol A35, 1987 p 3978.

12. Ba Enxu, et al., CHINESE JOURNAL OF LASERS, Vol 11, 1984 p 105.

High Power Sum Frequency Generation of 230.8-223.2 nm in BBO Crystal

40090010c Beijing WULI XUEBAO [ACTA PHYSICA SINICA] in Chinese Vol 39 No 2, Feb 90 pp 190-193

[English abstract of article by Lu Shiping [7627 1102 1627], Yuan Yiqian [5913 2022 6197] et al., of Anhui Institute of Optics and Fine Mechanics, Chinese Academy of Sciences, Hefei]

[Text] Continuously tunable second harmonic generation of 294.8-282.5 nm was obtained by a Q-switched YAG laser-pumped Rh.6G dye laser in a 45° cut β-$B_aB_2O_4$ (BBO) crystal. The output energy of the harmonic wave is approximately 8 mJ around 285 nm. The continuously tunable output over the range of from 230.8 to 223.2 nm was also obtained by the sum frequency mixing between the residual pump fundamental wave (1064 nm) and the second harmonic wave of the Rh.6G dye laser in another 45° cut BBO crystal. The sum frequency output energy is approximately 120 µJ around 226 nm, with a corresponding power peak of 12 kW. The key techniques of the sum frequency generation are indicated.

References

1. Chen, C., et al., SCIENTIA SINICA (Ser B), Vol 28, 1985 p 235.

2. Kato, K., IEEE J QUANT ELECT, Vol QE-22, 1986 p 1013.

3. Muchenheim, W., et al., APPL PHYS, Vol B45, 1988 p 259.

4. Shen, Y.R., "The Principles of Nonlinear Optics," New York, 1984, p 72.

Vector Scattering Theory, Experiments for Multilayer Optical Coatings

40090010d Beijing WULI XUEBAO [ACTA PHYSICA SINICA] in Chinese Vol 39 No 2, Feb 90 pp 194-203

[English abstract of article by Zhan Yuanling [2069 0337 7881] and Wang Li [3769 4539] of the Department of Physics, Nankai University, Tianjin]

[Text] A new method is presented for predicting the distribution of vector scattered fields of multilayer optical coatings. The scattering properties of film stacks with various interface cross-correlation models are discussed according to the statistical principles. The theory has been related to the familiar concepts of thin film optics, and simple results are obtained. It is shown theoretically that even though the optical parameters of the multilayer optical coatings are the same, the scattering losses can be quite different due to the different interface cross-correlations.

Measurements of the scattered field distribution of optical films have also been made, and from them the interface cross-correlations of the multilayer optical films are determined according to the vector scattering theory.

References

1. Eastmann, J.M., "Physics of Thin Films," Advances in Research and Development, 10, Academic Press, 1978.

2. Carniglia, C.K., OPT ENG, Vol 18, 1979 p 104.

3. Elson, J.M., APPL OPT, Vol 16, 1977 p 2872.

4. Gourley, S.J., Lissberger, P.H., OPT ACTA, Vol 26, 1979 p 117.

5. Bousquet, P., et al., J OPT SOC AM, Vol 71, 1981 p 1115.

6. Vook, R.W., OPT ENG, Vol 23, 1984 p 343.

7. Dirks, A.G., Leamy, H.J., THIN SOLID FILMS, Vol 47, 1977 p 219.

8. Guenther, K.H., APPL OPT, Vol 23, 1984 p 3806.

9. Maradudin, A.A., Mills, D.L., PHYS REV, Vol B11, 1975 p 1392.

10. Zhang Juhong, et al., "Programming In BASIC," Qinghua University Press, 1983.

11. Zhan Yuanling, et al., ACTA OPTICA SINICA, Vol 9, 1989 p 635.

RHEED Intensity Oscillations in Molecular Beam Epitaxy Growth of Ge, Si on Si Substrates

40090010e Beijing WULI XUEBAO [ACTA PHYSICA SINICA] in Chinese Vol 39 No 2, Feb 90 pp 237-244

[English abstract of article by Chen Keming [7115 0668 2494], Jin Gaolong [6855 7559 7893] et al., of the Laboratory of Surface Physics, Fudan University, Shanghai]

[Text] RHEED intensity oscillations during the MBE growth of Ge and Si on Si (100) and Si (111) substrates have been observed. It is revealed that a finite-thick buffer layer can improve the surface flatness of the Si substrates, and that the employment of a lower growth rate or growth interruption procedure can improve the crystal quality of the epilayers. During the growth of Ge and Si on Si (100), a single atomic layer mode RHEED intensity oscillation was observed along either the [100] or [110] azimuthal direction, which was due to the existence of the double domain (2x1)+(1x2) reconstruction on the surface. During the growth of Ge on Si (111) substrates, the RHEED intensity oscillation exhibited a bilayer mode along the [112] azimuth, but nonuniform periodicity along the [110] azimuth. The oscillations for continuously growing Ge on either Si (100) or Si (111) can exist up to an epilayer thickness of 6ML, which corresponds to the critical thickness of pseudomorphic growth of Ge on Si.

References

1. Dobson, P.J., et al., J CRYST GROWTH, Vol 81, 1987 p 1.

2. Kawamura, T., Maksym, P.A., SURF SCI, Vol 161, 1985 p 12.

3. Sakamoto, T., et al., APPL PHYS LETT, Vol 47, 1985 p 617.

4. Sakamoto, K., et al., JAPN J APPL PHYS, Vol 26, 1987 p 666.

5. Sakamoto, T., Hashiguchi, G., JAPN J APPL PHYS, Vol 25, 1986 p L78.

6. Aarts, J., et al., APPL PHYS LETT, Vol 48, 1986 p 931.

7. Jin Gaolong, et al., ACTA PHYSICA SINICA, Vol 38, 1989 p 394.

8. Chen Keming, et al., CHINESE JOURNAL OF SEMICONDUCTORS, Vol 9, 1988 p 435.

9. Hamers, R.J., et al., PHYS REV, Vol B34, 1986 p 5343.

10. Bevk, J., et al., APPL PHYS LETT, Vol 49, 1986 p 286.

END OF
FICHE

DATE FILMED
24 May 90